P514915.PDF [Page: 3 of 65]

Copy No. 1

DEFENCE R&D DÉFENSE

SUBMO3: A FREQUENCY DOMAIN SIMULATION TOOL FOR SUBMARINE MOTION IN WAVES, AND ITS USE WITH MANEUVERING MODELS

A. Field

ISE Research Limited

DEFENCE RESEARCH ESTABLISHMENT ATLANTIC

Contractor Report

DREA CR 2000-049

April 2000

National Defence Défense nationale

Cana

102-02556/

National Defence
Research and Development Branch

Défense nationale
Bureau de recherche et développement

DREA CR 2000-049

SUBMO 3: A FREQUENCY DOMAIN SIMULATION TOOL FOR SUBMARINE MOTION IN WAVES, AND ITS USE WITH MANEUVERING MODELS

A. Field

ISE Research Limited

Scientific Authority Kevin McTaggart
K. McTaggart

1gb14
Contract Number

April 2000

CONTRACTOR REPORT

Prepared for

Defence Research Establishment Atlantic

Centre de Recherches pour la Défense Atlantique

Canada

Submo3: A Frequency Domain Simulation Tool for Submarine Motion in Waves, and Its Use with Maneuvering Models

Adrian Field, ISE Research Limited

Abstract

This report summarizes the developments made to Submo2 resulting in the more recent version, Submo3. Particular changes include the addition of surge motion characteristics, and the ability to output exciting forces to a data file. These changes result in a complete 6 degree of freedom submarine motion model. The results from the software are validated in this work using an ellipsoid and Series 60 hull form, using Shipmo7 and existing literature. Specific use of the excitation force data file for the addition of wave forces and modelling to existing manoeuvring models, such as DSSP, is also detailed. The software code for wave excitation forces in the time domain has been developed and is presented. The procedures are verified by linear time domain simulation and results are compared with frequency domain results from Submo3 and Shipmo7. A method for frequency dependent radiation effects in the time domain is shown.

Résumé

Le présent rapport résume les améliorations apportées au Submo2 pour en arriver à la version plus récente, Submo3. Comme modifications précises on retrouve l'ajout de caractéristiques de mouvement de cavalement et la capacité d'envoyer des forces d'excitation dans un fichier de données. Ces modifications ont permis d'obtenir un modèle de déplacement de sous-marin à 6 degrés complets de liberté. Les résultats tirés du logiciel sont validés dans le présent ouvrage à l'aide d'une forme de coque ellipsoïde et de série 60, du Shipmo7 et de documents existants. Il est aussi question de l'utilisation précise du fichier de données de force d'excitation pour l'ajout de forces de vagues et de la modélisation en fonction des modèles de manœuvres existants, comme le DSSP. Le code de logiciel pour les forces d'excitation des vagues dans le domaine temporel a été mis au point et est présenté. Les procédures sont vérifiées par une simulation en domaine temporel linéaire et les résultats sont comparés avec les résultats du domaine des fréquences provenant de Submo3 et de Shipmo7. Une méthode pour les effets du rayonnement en fonction de la fréquence dans le domaine temporel est donnée.

Submo3: A Frequency Domain Simulation Tool for Submarine Motion in Waves, and Its Use with Maneuvering Models

Adrian I. Field
I.S.E. Research Ltd. (Contractor)
1734 Broadway St., Port Coquitlam, B.C., Canada

DREA CR 2000-049

Submo3: A Frequency Domain Simulation Tool for Submarine Motion in Waves, and its use with Manoeuvring Models

by

Adrian Field

EXECUTIVE SUMMARY

Introduction

DREA's simulation capability for maneuvering of underwater vehicles has been limited to calm water. For vehicles operating near the surface, wave effects can significantly influence vehicle motions. This report describes the prediction of underwater vehicle motions in waves and the inclusion of wave effects in maneuvering simulations.

Principal Results

The SUBMO program, which predicts motions of underwater vehicles in waves, has been upgraded to predict surge motions. The upgraded program also outputs wave excitation forces in the frequency domain. Subroutines have been developed to convert these excitation forces to the time domain, as required by maneuvering simulators. The predicted excitation forces are available for both regular and random seaways, and include the variation of submarine position with time. A preliminary validation study shows good agreement between motion predictions from the frequency and time domains.

Significance of Results

The influence of wave excitation forces can now be included in maneuvering simulations of underwater vehicles, resulting in more realistic predictions of vehicle motions. The current capability does not include wave radiation forces, which can be significant for vehicles at or near the free surface. If the current subroutines are incorporated into underwater vehicle maneuvering models, then extensive validation should be done to ensure the fidelity of the integrated software.

Future Plans

The developed software will be integrated into underwater vehicle maneuvering models. Required validation studies will be conducted to verify the results of the upgraded maneuvering models. Consideration will be given to including wave radiation forces.

Notation

TABLE 1.

Symbol	Description
A	Added mass
A_{ij}	Sectional added mass component
B	Potential damping
B^C_{ij}	Circulatory damping
B_{ij}	Potential damping component
Bm	Beam of vessel
B^V_{ij}	Viscous damping
C^C_{ij}	Circulatory stiffness
C_{Dfr}	Frictional drag coefficient
C_{Dfrf}	Roughness drag coefficient
C_{Ds}	Spray drag coefficient
C_{Dv}	Ventilation drag coefficient
C_{ij}	Potential stiffness
d	Water depth
F^C_i	Circulatory excitation force
F^D_i	Diffracted excitation force
F^E_i	Total excitation force
F_h	Froude number
F^I_i	Incident (Froude-Krylov) excitation force
g	Acceleration due to gravity
$H_{1/3}$	Significant wave height
h_j	Diffraction amplitude factor
k	Wave number
k_{11}	Lamb's coefficient of accession to acceleration
K_{ij}	Retardation integral kernel
k_x	Wave number component in 'x' direction
k_y	Wave number component in 'y' direction
L	Overall vessel length
M	Inertial matrix
m	Mass of vessel
{n}	Unit vector normal to hull
N_j	Unit vector component

TABLE 1.

Symbol	Description
P	Total pressure
Re	Reynolds number
S	Wetted surface of hull
T_p	Statistical peak wave period
T_ω	Energy averaged wave period based on frequency
WS	Wetted surface area
X, Y, Z	Body reference orthogonal axes
x, y, z	Inertial location components
Xe, Ye, Ze	Earth reference orthogonal axes
z_0	'Z' component of mean water level
z_{fs}	'Z' value as entered into Submo
α	Wave amplitude
α^*	JONSWAP spectra variable
β	Wave direction relative to vessel
ϕ_R	Radiative fluid potential
γ	JONSWAP spectra variable
η	State vector of pose and position
φ	Direction of vessel travel relative to inertial frame
φ_w	Direction of wave travel relative to inertial frame
κ	JONSWAP spectra variable
θ	Relative excitation component phase angle
ρ	Fluid density
σ	JONSWAP spectra variable
ω_0	Wave frequency
ω_e	Encounter frequency
ω_p	Peak wave frequency
ψ_j	Sectional potential
ψ_w	Direction of wave travel
ζ	Body reference velocity

Contents

Abstract ii

EXECUTIVE SUMMARY iii

Notation iv

Contents vi

1.0 Introduction 1

2.0 Surge Motion 1

2.1 Formulation 1

2.2 Validation 5

2.2.1 Ellipsoid 5

2.2.2 Series 60 11

3.0 Excitation Forces 16

3.1 Generation and Structure 16

3.2 Defined Wave Spectra 17

3.3 Time Domain Formulation in Translating Earth Axes 17

3.3.1 Time Domain Formulation for Earth Fixed Reference Frame 18

3.3.2 Radiation Effects 21

4.0 Time Domain Code Verification 22

4.1 Linear Time Domain Verification Theory 22

4.2 Results 24

5.0 Conclusion 34

6.0 Future Work 34

7.0 Appendix A - User Information for Subroutines 35

7.1 Subroutine wvamp(datafile,wf,alpha) 35

7.2 Subroutine wexfor(t,x,y,z,U,head,wf,alpha,fwave) 35

7.3 Subroutine irate(z,U,head,fcomp,pcomp) 36

7.4 Sample Wave Data File 36

8.0 Appendix B - Sample Verification Input Files 37

8.1 Ellipsoid Submo param.dat 37

8.2 Ellipsoid Submo geom.dat 37

8.3 Series 60 Submo param.dat 47

8.4 Series 60 Submo geom.dat 47

9.0 References 51

1.0 Introduction

Traditional submarine manoeuvring models and simulations are based on the deeply submerged operating condition. This assumes that there are no apparent frequency dependent effects, which for many cases is valid. However, there is increasing interest in near surface operating conditions due to mission objectives concerning surveillance, counter-measures, and intelligence. Accordingly, software code similar in theory to that developed for ships, in the frequency domain, has been developed for submarines. The drawback to simulation in the frequency domain is that the solution of the vehicle motion assumes a sinusoidal response having frequency equal to that of the exciting forces and no transient potential effects can be solved. In addition, frequency domain solutions are limited by the assumption of a steady forward speed. The goal of this work is to complete the frequency domain simulation in 6 degrees of freedom and use it as a stepping stone to time-domain models.

The Submo program performs frequency domain analysis of the motion of a submarine in waves based on strip theory [1]. Strip theory makes the assumptions of irrotational, and inviscid flow. Validity of strip theory requires that appropriate constraints must be met: operation at moderate speeds, vehicle has a slender body, and moderate sea states are present. This theory in application to submarines has been validated extensively [2], and produces reasonable results. The theory is based on potential flow, and superposition such that components of the flow are summed. The fluid potential is composed of 3 constituents: radiation, incident, and diffracted potential functions. From potential theory, it is apparent that the incident (Froude-Krylov) exciting forces due to surface waves diminish exponentially with depth, and the diffracted wave effects correspondingly. Wave radiation forces are usually small for submersibles [3], and are usually not considered for deep submergence. The calculation and modelling of these three components will be addressed here for surge motion in the frequency domain, and for all motions in the time domain.

2.0 Surge Motion

2.1 Formulation

The surge mode, similar to the other modes of motion, satisfies the equations of motion for a rigid body in a fluid. In Submo, the motions in various modes are considered decoupled. Due to lateral symmetry, lateral motions are decoupled from vertical. Sway, roll, and yaw are solved as one set, while heave and pitch are solved as another. It is assumed that surge motion coupling with heave and pitch is small. Surge motion, will be calculated as its own set, although the solution of the complete, complex linear equations is performed in a matrix oriented, coupled manner. The time domain equations of motion are [4]:

$$([M]+[A])\{\ddot{\eta}\}+([B]+[B^V]+[B^C])\{\dot{\eta}\}+([C]+[C^C])\{\eta\} = \{F^I\}+\{F^D\}+\{F^C\} \qquad (1)$$

where the radiative added mass terms are composed of the added mass [A] and damping [B], while the viscous terms are given by $[B^V]$, and the circulatory effects are found in $[B^C]$, and $[C^C]$. The excitation force is the sum of the incident wave forces $[F^I]$, the diffracted wave forces $[F^D]$, and the circulatory lift forces $[F^C]$. All the forces and motions are given with respect to the translating earth axes, following the mean body trajectory as in Figure 1.

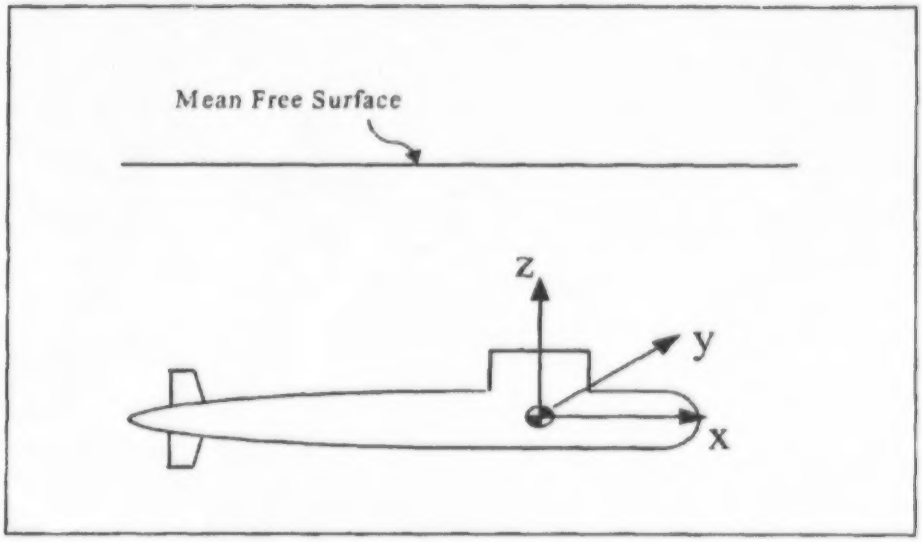

Figure 1: Axis Based on Mean Body Trajectory.

For the case of surge motion, all circulatory effects are neglected, and for preliminary study, diffracted wave buildup, such as bow wave effects will be neglected. Also, there are no stiffness effects associated with forward motion. If strip theory is valid, and thus a slender body exists, the change in potential in the x direction is small,

$$\frac{\partial \phi_R}{\partial x} \equiv 0 .$$

So the use of strip theory is not possible for calculation of the surge hydrodynamic coefficients. Surge potential damping is due to the energy needed for the generation of surface waves, or wave-making drag. Computation of wave-making drag is possible using potential theory [5], but is extremely involved. For this approach wave drag will be neglected due to its decreased relative magnitude by depth in relation to viscous damping. This leaves:

$$(m + A_{11})\ddot{\eta}_{11} + B_{11}^{V}\dot{\eta}_{11} = F_1^I(t) \qquad (2)$$

Transferring this expression into the frequency domain, assuming both the excitation and response is a sinusoidal function having equal frequency, due to steady oscillations,

$$(-\omega_e^2(m + A_{11}) + i\omega_e(B_{11}^{V}))\{\eta_{11}\} = F_1^I(\omega_e) \qquad (3)$$

In this way, for each given frequency, the corresponding response is found in complex form, providing amplitude and phase information. The calculation of surge motion in no way affects the calculation of the other modes of motion, neither does it interfere with Submo's iteration methods for roll motion.

In order to find the information relevant to solving eq. 3, the added mass, viscous damping and Froude-Krylov excitation forces must be found for the surge direction.

The added mass is found using the relation:

$$A_{11} = km, \tag{4}$$

where k, the Lamb coefficient of accession to inertia is found by,

$$k = 0.6\frac{B_m}{L}. \tag{5}$$

Here, m is the mass of the vehicle, B_m, the midship beam, and L the overall length of the vehicle. The midship beam is found using the maximum submerged beam at midship. So, for vehicles having a length to beam ratio of 6 to 10, k ranges from 0.06 to 0.1. This relationship is not frequency dependent and will have large error for low frequencies.

The calculation of the viscous damping is performed by summing the effects of the various hull components. The total damping is found by:

$$B_{11}^{V} = \frac{1}{2}\rho U \times TWA \times \sum_{n=1}^{N} C_{D_n}(\Delta A), \tag{6}$$

where N is the number of components contributing to viscous drag, C_D is a component's drag coefficient, and ΔA is the nominal area of the component in question non-dimensionalized by the total wetted hull surface area, TWA.

Hull skin friction drag component is found from the I.T.T.C 1957 relation:

$$C_{D_{ff}} = \frac{0.075}{(\log((Re)-2))^{-2}}, \tag{7}$$

this relation is based on wetted surface area and was developed based on the more complicated Schoener relation:

$$\log(ReC_{D_{ff}}) = \frac{0.242}{\sqrt{C_{D_{ff}}}}. \tag{8}$$

A fouling or roughness drag effect, also based on wetted surface area, is present based on A.T.T.C. 1947 findings, resulting in,

$$C_{D_{fr}} = 0.0004. \tag{9}$$

For most clean hulls this value produces good results.

The drag incurred due to the foils is found using Aucher's [6] general value of,

$$C_{D_f} = 0.01 , \tag{10}$$

for low aspect ratio foils, having square wing tips and not exceeding a sweep angle of 25 degrees. This value is based on the foil surface area.

As the simulation examines near surface operation, there is a large chance that either the sail, periscope or a fin pierces the surface. Submo2 allows for hydrostatic surface piercing effects, and if surface piercing, only uses the wetted geometry for calculation of added mass and damping. Foils, if included in the model, have the options of,

1) Being incorporated into hull geometry for use in 2-dimensional added mass and damping calculations, and hydrostatic calculations.

2) Having foil circulatory effects included in the exciting forces.

Irrespective of these options, foils are always included for calculation of roll damping, and unsteady viscous lift. The first option mentioned above requires an extremely large number of segments in the 2-dimensional plane as well as a high density of stations in the region of the foil in order for a realistic adoption of the foil in the hull geometry. Two points of interest arise from this observation. First, if a foil is to be used as part of the hull geometry, then the surface piercing effects should be found after this stage. Second, as a foil or sail may be surface piercing, there will exist ventilation, and spray drag which could contribute greatly to the overall body drag [7]. Methods for calculation of these coefficients are available [8]. A general description of spray drag is given as,

$$C_{D_s} = 0.24 , \tag{11}$$

based on thickness, for slender struts. And ventilation drag can be found by,

$$C_{D_s} = \left(\frac{t}{c}\right) / F_h^2 , \text{ where Fh is Froude number based on submersion depth.} \tag{12}$$

The contribution of these effects has not been included in the code for Submo 3.

Finally, the Froude-Krylov surge forces on the body must be found. Linear wave theory is used to assume a sinusoidal wave profile and corresponding pressure potential field. The contribution of submarine diffraction forces is assumed to be negligible for surge. The forces on the hull are given by,

$$\{F\} = \int_{WS} \int (P \cdot \{n\}) dS , \tag{13}$$

where WS is the wetted hull surface, $\{n\}$ is the unit vector normal to the surface and P is the wave pressure field given by,

$$P = (\alpha\rho g)e^{-ik(x\cos\beta + y\sin\beta)}e^{k(z-z_0)}. \tag{14}$$

So, looking only at the surge component, and combining the two equations,

$$F_1^I = \int_{Stern}^{bow} (\alpha\rho g)e^{k(z-z_0)}e^{-ik(x\cos\beta + y\sin\beta)}\frac{dA}{dx}dx. \tag{15}$$

This gives a similar solution to that for ship surge motion [9]. In this manner, all the hydrodynamic components are determined for the surge direction, and the solution of the equations of motion (eq. 1) can be achieved.

2.2 Validation

In order to ensure that the correct methodology and programming was carried out, validation of the modified Submo code was performed. As a preliminary check, the geometries for comparison were viewed using the "genps2.f" code which generates post-script format files. As some geometries were not compatible with this code, minor modifications were made to incorporate a wider range of hull shapes, and smoother grid formation. This file is called "genps3.f". The following describes two validation sets. As Shipmo requires equally spaced station locations, whereas Submo is able to integrate variably spaced station data, even station placement was used for comparison.

2.2.1 Ellipsoid

The geometry for an ellipsoid was used due to its definite characteristic shape. The following details were used: a length to beam ratio of 7, beam to draft ratio of 2, and a total of 19 stations. An actual length of 7 meters was used. The mean water line was assumed at the plane of symmetry of the ellipsoid. It is interesting to note that Shipmo has the option of a transom stern, that is, rather than adding a point aft of the last station, the last station is used as the aft of the ship. Submo, on the other hand, automatically enters two additional hull locations, one at the bow and one at the stern using the overall length of the vessel. Submo uses the last user entered station for speed dependent strip theory calculations, which is only valid for 'bluff' type sterns. The geometry, as entered into Submo is shown in Figure 2, note that "genps" does not include the additional end stations in visualization.

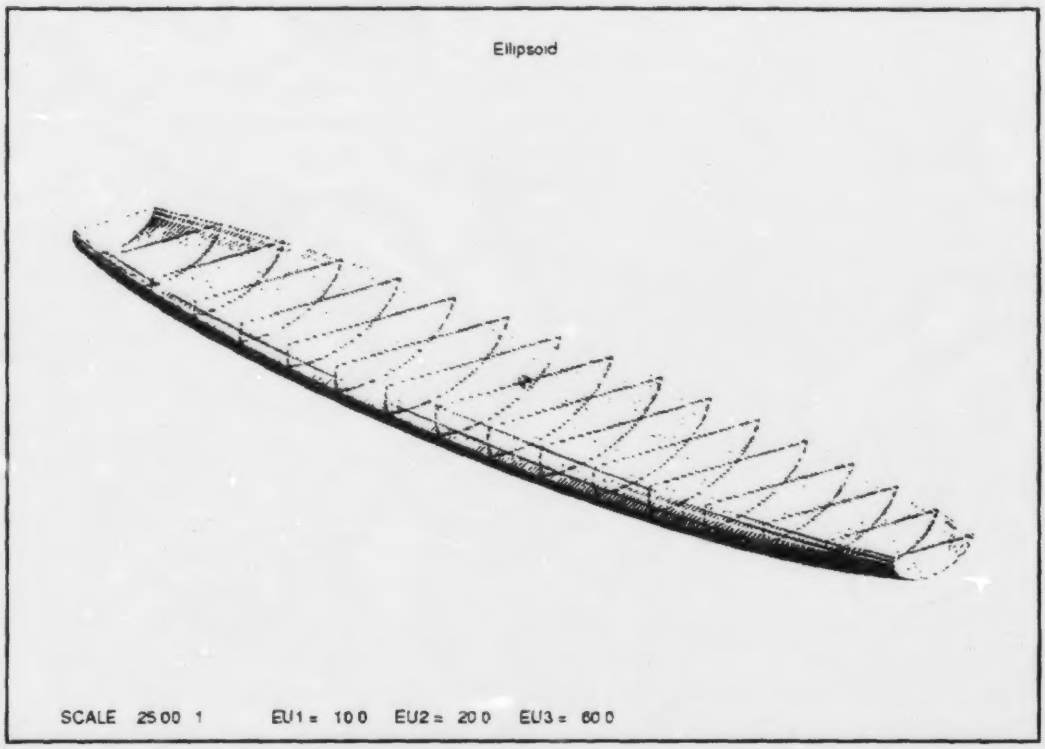

Figure 2: Ellipsoid Geometry

From the visualization it is apparent that for correct modelling of an ellipsoid a higher station density near the end points would be more appropriate, however, as similar geometries were used for both programs, this is used for comparative purposes. It is important to note that a higher station density is generally needed before as well as after a large change in area, as Submo uses quadrature integration. Two speeds and three headings were compared and the results are shown in Figures 3-10. In these figures, translational motion amplitude is made non-dimensional by wave amplitude (α), rotational motion amplitude by encounter wave slope ($(2\pi/\omega)^2*\alpha g$), whereas encounter frequency is made non-dimensional by hull length and gravity ($(L/g)^{0.5}$). This convention is maintained in all relevant figures.

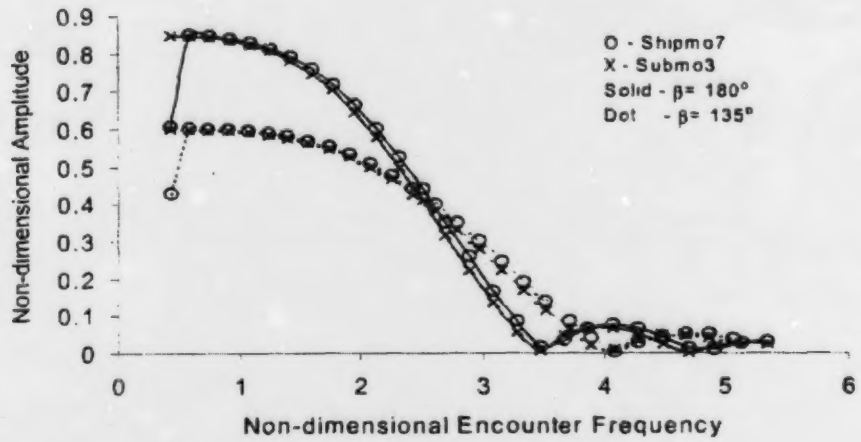

Figure 3: Ellipsoid Verification, Surge Motion Amplitude, Fn 0

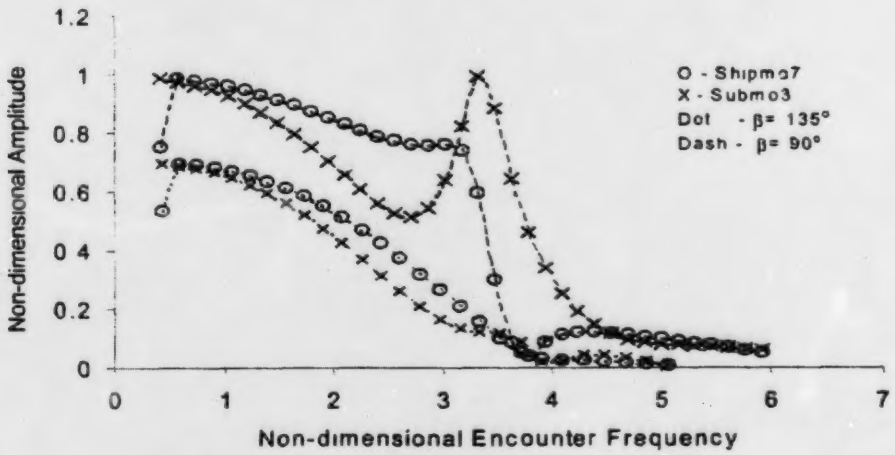

Figure 4: Ellipsoid Verification, Sway Motion Amplitude, Fn 0

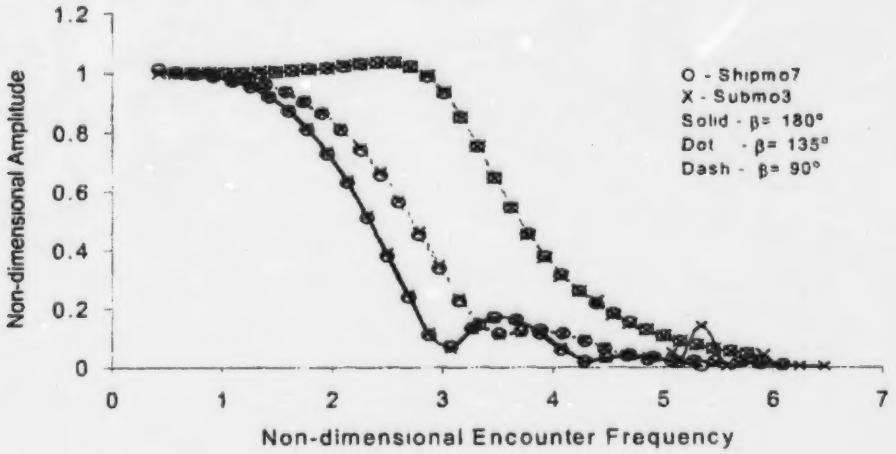

Figure 5: Ellipsoid Verification, Heave Motion Amplitude, Fn 0

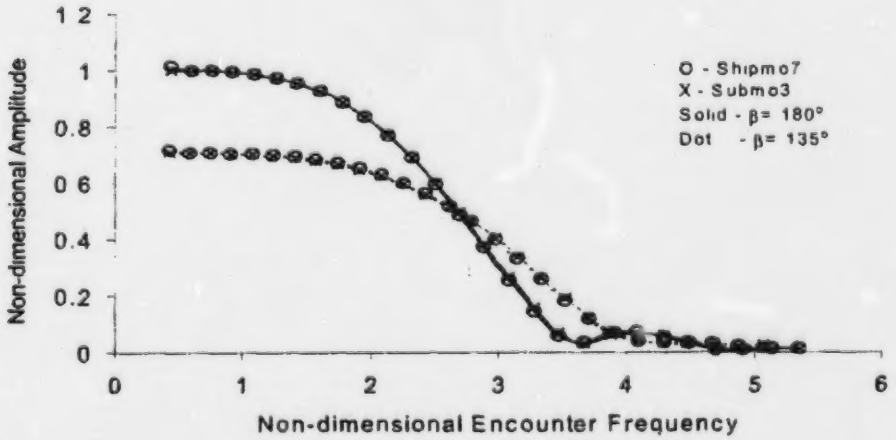

Figure 6: Ellipsoid Verification, Pitch Motion Amplitude, Fn 0

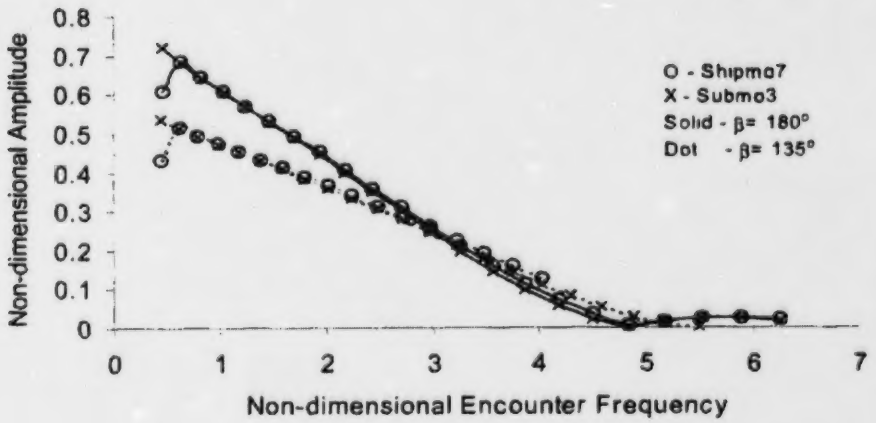

Figure 7: Ellipsoid Verification, Surge Motion Amplitude, Fn 0.2

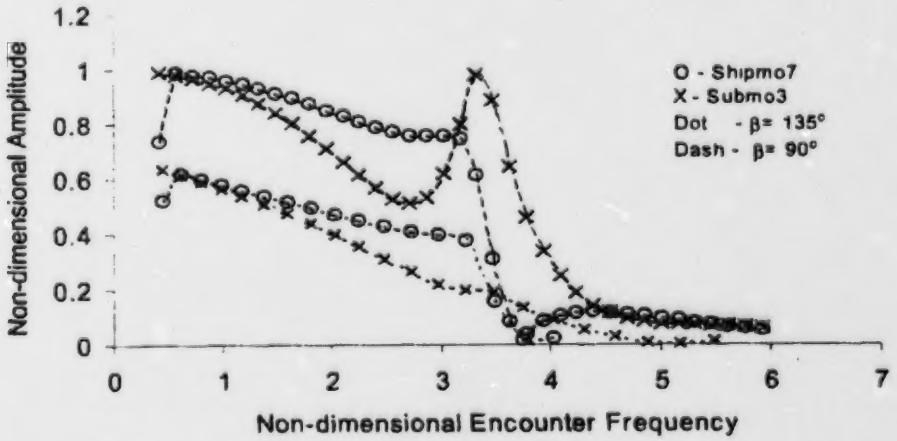

Figure 8: Ellipsoid Verification, Sway Motion Amplitude, Fn 0.2

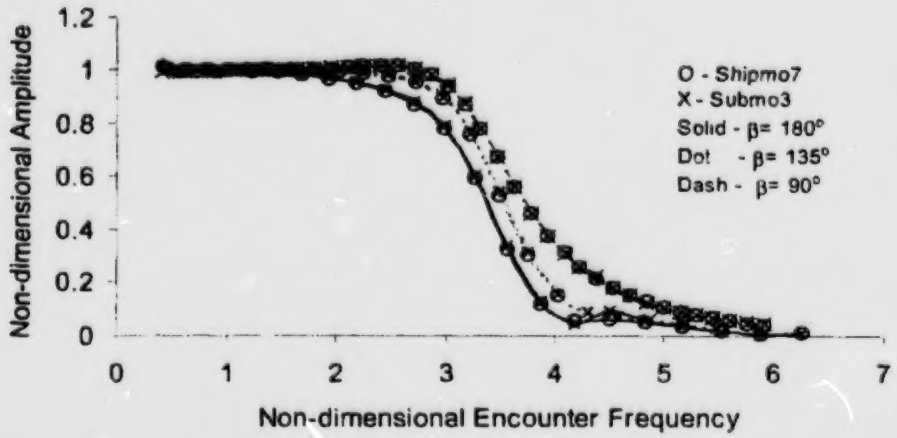

Figure 9: Ellipsoid Verification, Heave Motion Amplitude, Fn 0.2

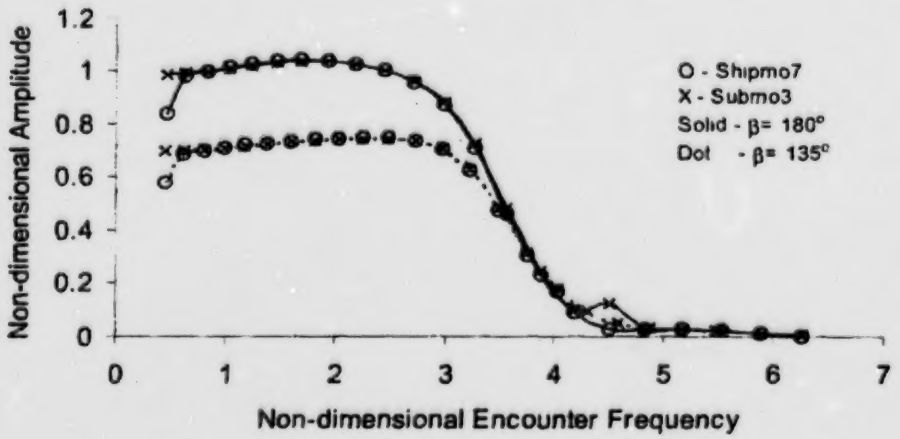

Figure 10: Ellipsoid Verification, Pitch Motion Amplitude, Fn 0.2

The figures show that excellent agreement is found between the two programs for both speeds and all headings. These results are expected as similar algorithms were used in both software packages. The only difference of note is that for sway characteristics. For the 90 degree heading, Submo appears to predict a peak in response. This could be an either an actual resonant frequency or a

numerical singularity involved in the solution. It should be noted that improved methods are used in Shipmo7 for hydrodynamic calculation [11]. From these results, surge verification data for Shipmo should also be applicable to Submo.

2.2.2 Series 60

Since the adoption the standardized Series 60 hull shapes [12], extensive testing and comparison has been performed using these forms. In this way new numerical formulations can be readily checked against previous experimental and mathematical results. For the case of the Series 60 hull form, comparison with a previous numerical method [13] was done. The hull form having a block coefficient of 0.6 was used to ensure correct comparison, and an actual length of 3.05 meters was used. The corresponding Submo geometry is shown in Figure 11.

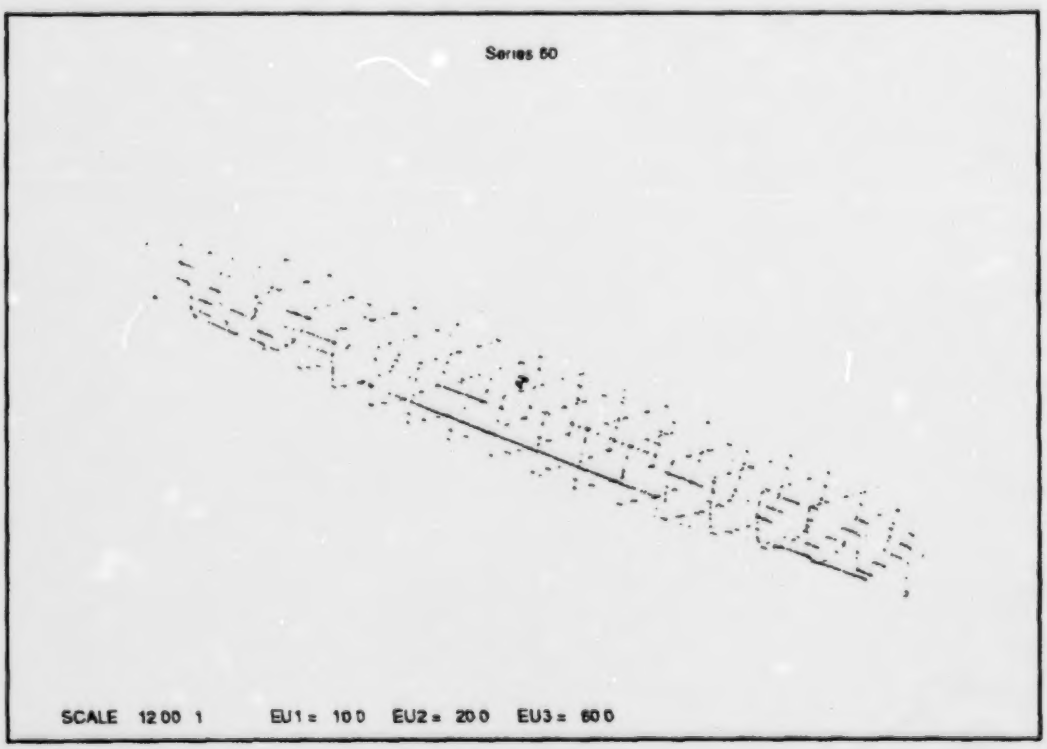

Figure 11: Series 60, 0.6 Hull Form Geometry

Note in this figure the sharp edges in the midsection of the ship. These 90 degree segments cause difficulty for the numerical solution of the hydrodynamic coefficients. It was found that any sectional geometry having sharp corners, caused warning flags to appear by the Submo in the calculation of roll-sway damping terms.

The results of the Series 60 comparison are shown in Figures 12-19.

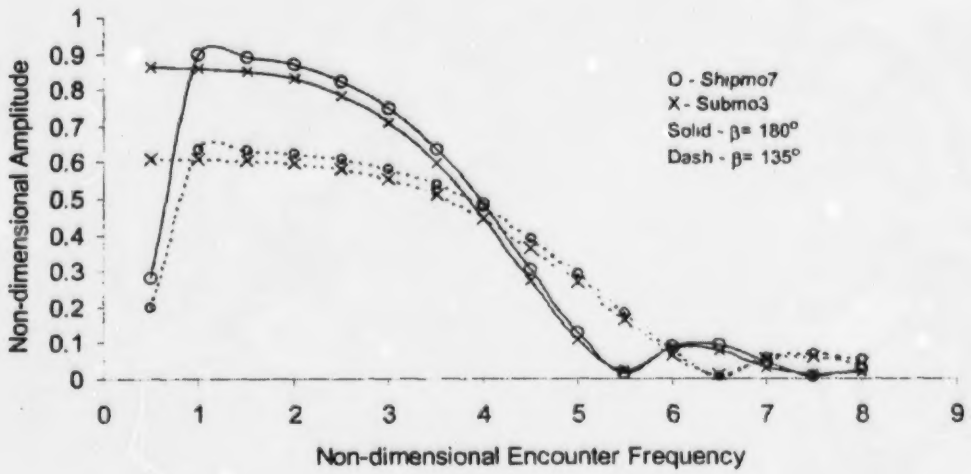

Figure 12: Series 60 Validation, Surge Motion Amplitude, Fn 00

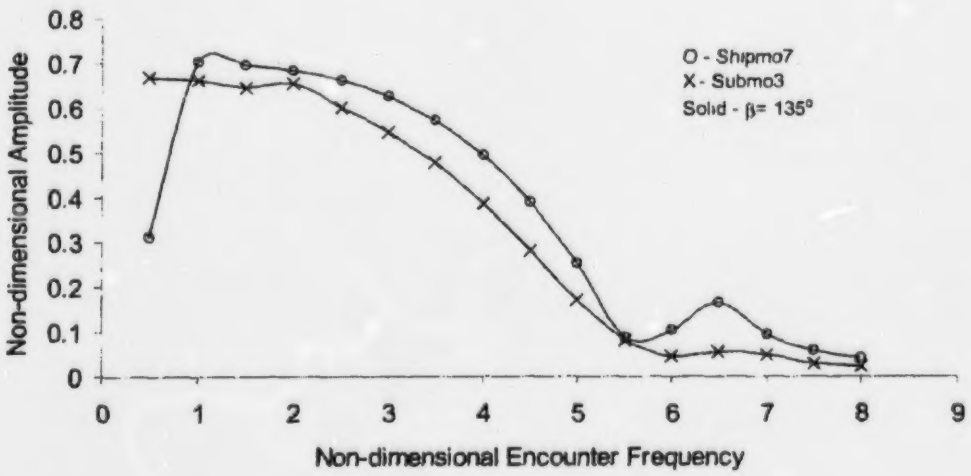

Figure 13: Series 60 Validation, Sway Motion Amplitude, Fn 0

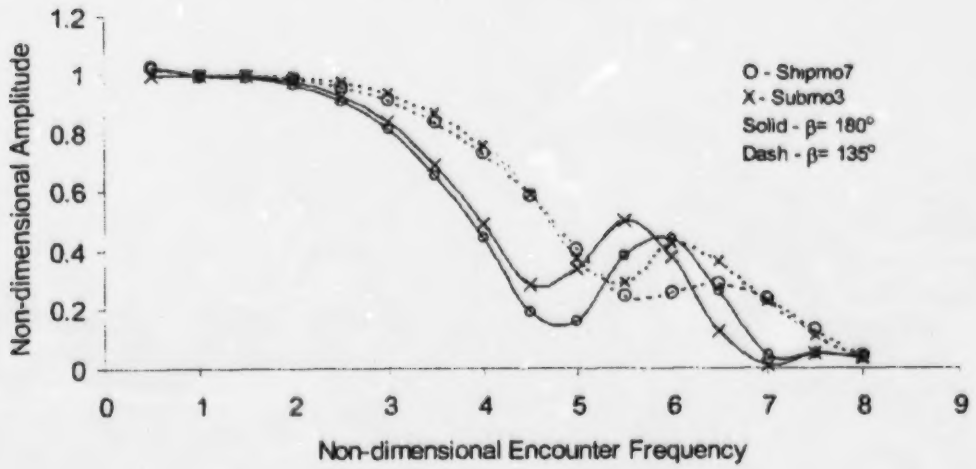

Figure 14: Series 60 Validation, Heave Motion Amplitude, Fn 0

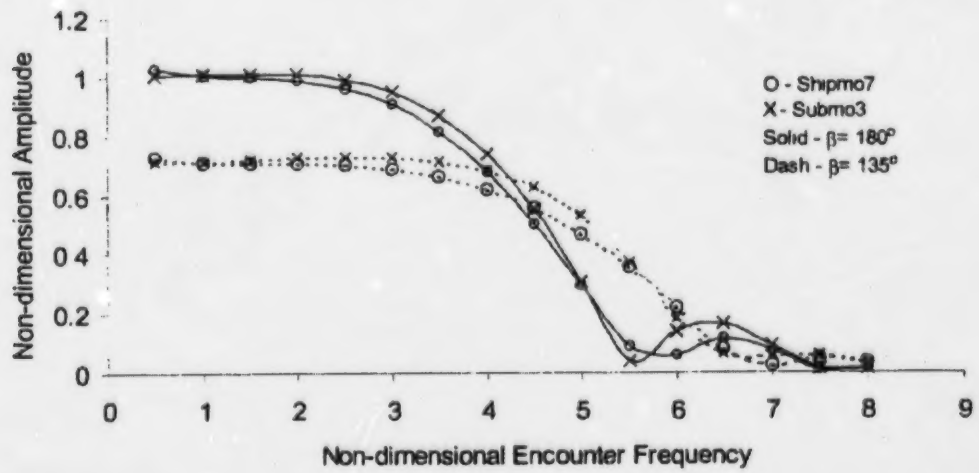

Figure 15: Series 60 Validation, Pitch Motion Amplitude, Fn 0

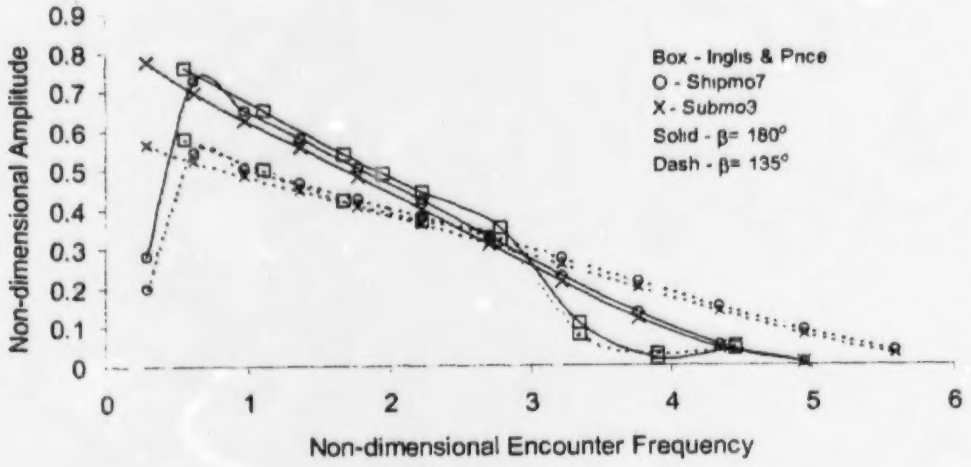

Figure 16: Series 60 Validation, Surge Motion Amplitude, Fn 0.2

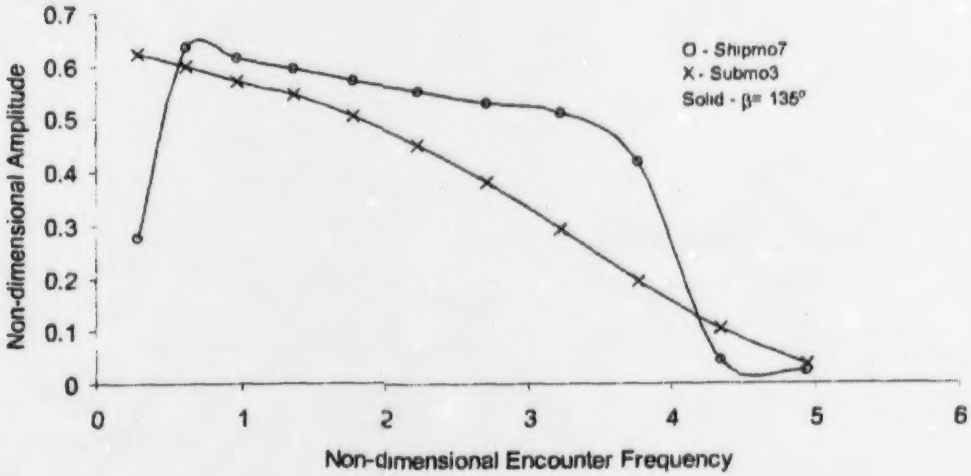

Figure 17: Series 60 Validation, Sway Motion Amplitude, Fn 0.2

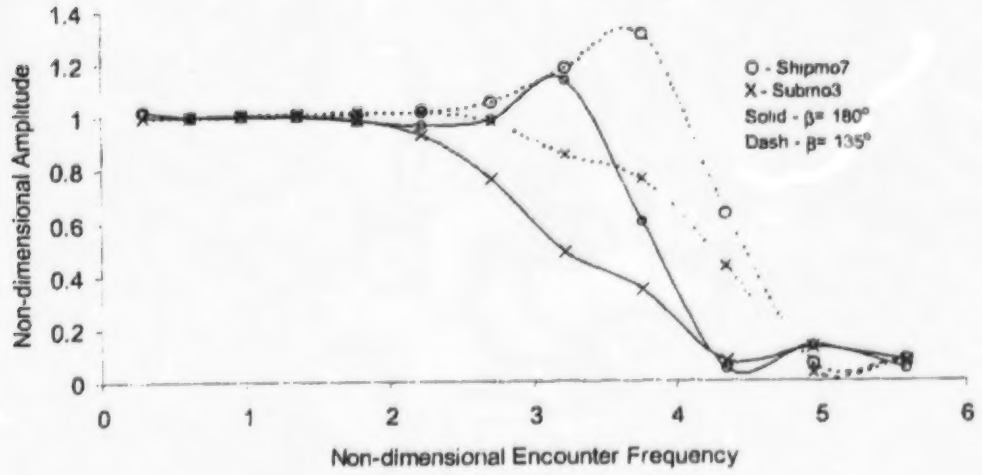

Figure 18: Series 60 Validation, Heave Motion Amplitude, Fn 0.2

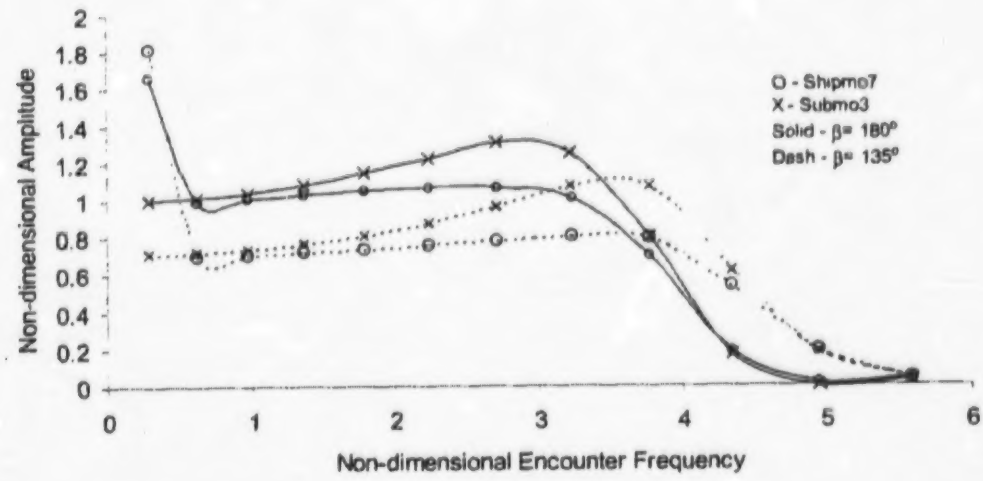

Figure 19: Series 60 Validation, Pitch Motion Amplitude, Fn 0.2

The figures show good agreement for the zero forward speed case and a noticeable difference for a Froude number of 0.2. Note that head wave conditions are denoted by $\beta = 180^0$. It appears that Submo tends to overpredict reponses in pitch and underpredict in heave. This could be largely due to the strip theory calculations, as the transom stern speed dependent term can be large. There is

also a slight difference in the reponse predicted for surge by Submo in relation to the literature. This difference is seen at 3.5 rad/sec as shown in Figure 16, and is likely because of diffraction effects which are not included by Submo, and which become important for higher frequencies. For head seas, the theoretical limit for low frequency response is 1, in deep water. This also provides a good comparison, although it is a theoretical limit using potential flow theory. Realistic values for low frequency response are often lower than this [14], which lends to the credibility of the validation here.

3.0 Excitation Forces

3.1 Generation and Structure

The total exciting forces, as shown by eq. 1, are comprised of the incident, diffracted and circulatory forces. Calculation of the incident forces is described by eqs. 13-15. Realization of the diffracted forces is slightly more involved and is shown here using strip theory. The sectional diffraction exciting force amplitudes are given [15] as,

$$h_j(x) = \rho\alpha\omega_0 \int_{C_x} (iN_3 + N_1\cos\beta + N_2\sin\beta) \times e^{-iky\sin\beta} e^{k(z-z_0)} \psi_j(y,z)dl, \quad j=2,3,4 \tag{16}$$

N_j are the unit normal vectors in each of the principle directions, and ψ, the sectional potential function is found using the Haskind relations. The integral is done about the circumference of the section. These amplitudes are then used in the integration of the diffraction forces along the length of the hull,

$$F_{Dj} = \int_L e^{-ikx\cos\beta} h_j(x)dx, \quad j=1,2,3,4 \tag{17}$$

$$F_{D5} = -\int_L e^{-ikx\cos\beta}\left(x + \frac{U}{i\omega_e}\right)h_3(x)dx, \text{ and} \tag{18}$$

$$F_{D6} = \int_L e^{-ikx\cos\beta}\left(x + \frac{U}{i\omega_e}\right)h_2(x)dx. \tag{19}$$

As previously mentioned, the diffraction forces for surge in Submo are assumed to be zero, however, the incorporation of eqs. 16-17 would be straightforward due to the existing structure and computation performed by the code.

Details of the calculation of the circulatory effects can be found in related literature [4], and will not be covered here. Computation of the exciting forces is performed for each heading, speed, mode, and frequency in Submo. The resulting forces are given in reference to the translating earth axes as shown in Figure 1.

Specific validation of excitation forces generated by Submo has been done. Comparison was made with experimental data for a range of speeds, depths, and headings. However, only the magnitudes

of these forces were validated and only for specific cases. To be confident of the theory presented here, further validation of phases of Submo excitation forces, as well as a wider range of headings should be completed.

3.2 Defined Wave Spectra

Only two wave spectra are defined in Submo2, the Pierson-Moskowitz and Bretschneider spectra. As the two are quite similar, this limits the range of possible sea conditions available for study using Submo. The JONSWAP spectra has been added to Submo3 for more flexibility. The code is consistent with Shipmo [19], and uses the formulation for a three parameter spectrum:

$$S(\omega) = \alpha^* H_{1/3}^2 \frac{\omega_p^4}{\omega^5} \exp\left(-1.25\frac{\omega_p^4}{\omega^5}\right)\gamma^{\kappa} \tag{20}$$

where, (21)

$$\alpha^* = 0.0624/(0.23 + 0.0336\gamma - 0.185/(1.9 + \gamma)) \tag{22}$$

$$\kappa = \exp\left(-\frac{(\omega - \omega_p)^2}{2\sigma^2\omega_p^2}\right) \tag{23}$$

and, (24)

$$\sigma = 0.07, \text{ for } \omega \le \omega_p \tag{25}$$

$$\sigma = 0.09, \text{ for } \omega > \omega_p$$

For the two parameter spectra in Submo, gamma is set to 3.3. The equivalent of this formulation has been input in the time domain files described in the following sections.

3.3 Time Domain Formulation in Translating Earth Axes

Typically a manoeuvring model uses time domain equation of motion as in eq. 1, however, the transformation of this equation from the frequency domain representation,

$$(-\omega_e^2([M] + [A]) + i\omega_e([B] + [B^V] + [B^C]) + ([C] + [C^C]))\{\eta\} = \{F^I\} + \{F^D\} + \{F^C\}, \tag{26}$$

is only straightforward for single frequency motions. Let the sum of the excitation forces be given for each mode as:

$$F^E_j = F^I_j + F^D_j + F^C_j, \quad j = 1, \ldots 6 \tag{27}$$

Complex forcing functions for a vehicle have phases relative to when the wave crest is aligned vertically with the vehicle centre of gravity. As the ship may not necessarily be symmetric in all

planes, there may exist a phase shift not only in the response of the vehicle, but also in the forcing function. This total complex force can be expressed as,

$$F^E_j(\omega_e) = \left|F^E_j\right| e^{i\theta_j}, \tag{28}$$

where, θ_j, is the phase shift of the forcing function, and $|F^E_j|$, is now the amplitude of the forcing function. Adding the time domain component to eq. 28,

$$F^E_j(\omega_e) = (F^E_j e^{i\theta_j} e^{i\omega_e t}) \tag{29}$$

and taking the real portion of the expression as shown,

$$F^E_j(t) = \left|F^E_j\right| \cos(\omega_e t + \theta_j). \tag{30}$$

If eq. 30 is the excitation force for one frequency and the principle of superposition holds, then the total wave excitation force for the collection of all frequencies exists as the sum,

$$F^E_j(t) = \sum_{n=1}^{N} \left|F^E_{jn}\right| \cos(\omega_{e_n} t + \theta_{jn}). \tag{31}$$

The description of a sea state as the sum of linear single frequency waves is conventional [16], and various spectra have been developed to this end. The selection of N is critical and it is suggested [17], that N should be greater than 30 for good representation of sea states. This value depends on the ratio of wavelengths within the spectral bandwidth to the geometry of the vehicle, typically the dimension of the length of the vehicle.

3.3.1 Time Domain Formulation for Earth Fixed Reference Frame

In the previous section eq. 30 was shown as the time domain representation of the exciting forces. This expression is true for a given forward speed, relative wave heading, and depth, and the values for eq. 31 are found accordingly. In manoeuvring models, however, the vehicle is able to travel a given trajectory which may cause these conditions to change. For a good representation of the exciting forces in the time domain, the range of operating speeds, headings, and number of frequencies, as mentioned previously, must be chosen to span the range of simulation appropriately. In Submo, it is possible to enter a range of speeds, headings, and frequencies in the file "inpt.dat" for a single execution of the software. Only one depth is entered, z_{fs}. The corresponding forcing data can be output to a file "fao.dat".

Submo3 is able to use "inpt.dat" files designed for Submo2, but no excitation force data is output. For the generation of "fao.dat", one line is added to the end of "inpt.dat" with an integer flag "0" for no output, or "1" for output in "fao.dat".

The file "fao.dat" is generated in the following format:

Number of Speeds	*Number of Headings*	*Number of Frequencies*					
flag = "a"	*Speed 1*	*Heading 1*	*Depth*				
flag = "c"	frequency 1	Mode 1 Re Excit	Mode 1 Im Excit	...	Mode 6 Re Excit	Mode 6 Im Excit	Wave Height
flag = "c"	frequency 2	Mode 1 Re Excit	Mode 1 Im Excit	...	Mode 6 Re Excit	Mode 6 Im Excit	Wave Height
flag = "c"	frequency 3	Mode 1 Re Excit	Mode 1 Im Excit	...	Mode 6 Re Excit	Mode 6 Im Excit	Wave Height
flag = "c"	frequency 4	Mode 1 Re Excit	Mode 1 Im Excit	...	Mode 6 Re Excit	Mode 6 Im Excit	Wave Height
flag = "c"	frequency 5	Mode 1 Re Excit	Mode 1 Im Excit	...	Mode 6 Re Excit	Mode 6 Im Excit	Wave Height
flag = "c"	frequency 6	Mode 1 Re Excit	Mode 1 Im Excit	...	Mode 6 Re Excit	Mode 6 Im Excit	Wave Height
flag = "c"	frequency 7	Mode 1 Re Excit	Mode 1 Im Excit	...	Mode 6 Re Excit	Mode 6 Im Excit	Wave Height
flag = "c"	frequency N	Mode 1 Re Excit	Mode 1. Im Excit	...	Mode 6 Re Excit	Mode 6 Im Excit	Wave Height
flag = "a"	*Speed 1*	*Heading 2*	*Depth*				

TABLE 2. Wave Exciting Force Database File Layout.

Both the real and imaginary portions of the excitation force are output, and are non-dimensionalized by the wave height. The wave height is also given in the last column. Problems at low and high frequencies are encountered if the wave height used is small or zero, due to division by "zero". As Submo3 develops spectral data using one of 3 methods, either the peak wave period must be approximately greater than 7 seconds, or the range of wave frequencies must be greater than 0.5 rad/s. This problem is not particular to the current modifications in Submo but also occurs in the presentation of non-dimensional results. This must be taken into account when constructing a complete range of data in the database file "fao.dat". The overall problem could be overcome by various methods but will not be discussed here.

The file size of "fao.dat" for 17 speeds, 24 headings, and 37 frequencies is approximately 2.6 megabytes. The file is generated in ASCII text format and can be viewed or modified in any text viewer. No changes are necessary for the use of "fao.dat" with the following time domain subroutines.

Three subroutines have been written in Fortran 90, for the access and construction of wave forces in the time domain. The subroutines are generic in nature and can be included in any FORTRAN time-step based simulator such as DSSP [18]. These are as follows:

Subroutine wvamp

The subroutine wvamp is called once, at the start of a simulation. This subroutine loads the file "fao.dat" into an array. The procedure then finds the magnitude and phase of the complex data. A wave spectrum is developed based on information input from the manoeuvring model. Four spectra are presently available: 1 - regular wave, for which a wave height and period are required, 2 - Pierson Moskowitz requiring significant wave height and average wave period, 3 - Bretschneider spectra requiring significant wave height and average wave period, or 4 - the two parameter JONSWAP spectra requiring significant wave height and average wave period [19]. The subroutine also reads the principle direction of wave travel (Figure 20), φ_w, as long crested seas are assumed.

The method of random wave phase difference [20] is used to realize the spectrum. A random phase, θ_{0n}, is generated for each wave frequency. The seed for random phase generation is variable and must be given for every simulation. The seed can be changed by an input parameter.

Subroutine wexfor

At every time step, the current position (x, y, z), heading (φ), and time, is required by the subroutine wexfor as shown in Figure 20. The time step can be variable and should be less than 0.85% of the average wave period for smooth results. The procedure calculates and returns the wave excitation force at each call. It is important to note that the forces given are based on a mean body reference frame as shown in Figure 1. Excitation forces as a function of time are shown in eq. 31, for fixed conditions. The definition of wave encounter frequency:

$$\omega_e = \omega - \frac{kU}{g}\cos(\beta), \tag{32}$$

and the identity cos(a)=cos(-a) are combined with eq. 31.

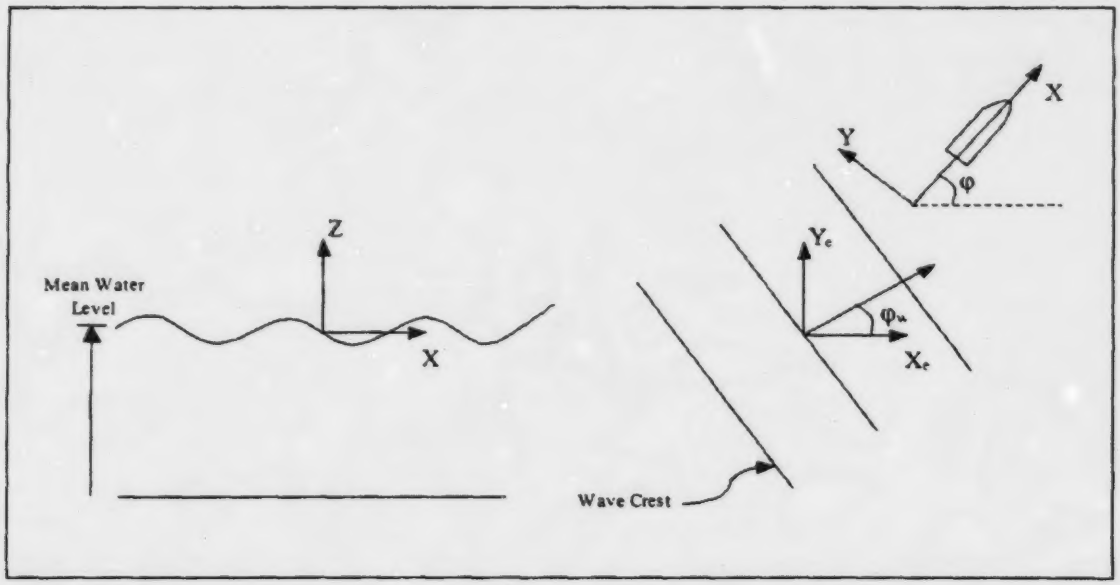

Figure 20: Definition of Ship and Wave Orientation in Earth Fixed Reference Frame.

For changing location, speed and heading, the following expression is found and utilized:

$$F^E_j(t) = \sum_{n=1-N} \left\| F^E_{jn}(U, \beta, z) \right\| \cos(-\omega_n t + k_x x + k_y y - \theta_{jn} + \theta_{0_n}) \tag{33}$$

Here, $k_x = k\cos(\varphi_w)$, and $k_y = k\sin(\varphi_w)$. The phase for each frequency and mode is different due to the initial random phase offset, θ_{0n}, and the modal offset, θ_{jn}, respectively. The angle in the trigonometric functions is the absolute direction of wave travel as shown in Figure 20. The variable $\beta = \varphi - \varphi_w$, is the relative wave angle with respect to the vessel and is consistent with Submo. If this value is negative, it is corrected to lie between 0 and 360 degrees. Both the principle sea direction and instantaneous heading must be within 0 to 360 degrees. The values for the magni-

tude and phase of the forcing function are found by calling the last subroutine, "intfor". Wexfor performs the calling of the interpolation procedure.

Subroutine intfor

This last procedure is called by wexfor, at each time step to interpolate in the data array. Before interpolation, the instantaneous speed and relative heading values are checked with the range of values in the data array. If outside the range of speeds or headings, either the highest or lowest value is used and an error message is output to the screen.

Once checked, the heading and speed are used to find 4 matrices of data bounding the given values. Using 2 dimensional linear interpolation, the matrix of modes and frequencies corresponding to the given heading and speed is found. Note: at least two speeds and headings are required for interpolation. As depth effects are known, a depth correction factor can found by,

$$\mathbf{dfact} = \frac{e^{k(z(t)-z_0)}}{e^{k(zfs)}} \tag{34}$$

where zfs is the value for depth used in Submo to calculate "fao.dat", z(t) is the time dependent z location in simulation, and z_0 is the mean water level in simulation. The value for z_0, is assumed zero as per Figure 20. This relationship assumes a large wavelength to beam ratio. Each frequency is corrected with a separate factor. The final interpolated magnitude and phase information matrices are passed back to wexfor.

3.3.2 Radiation Effects

The radiation hydrodynamic terms shown in eq. 1 when used in a manoeuvring model are usually the infinite frequency terms associated with deeply submerged operation. The infinite frequency added mass term may be found using conventional theories [21]. The damping effects are more complicated to include and usually potential damping is not considered. So, for a general manoeuvring model, only viscous and circulatory damping are considered. Potential damping is the damping caused due to energy dissipated to wave generation. The frequency dependent radiative terms can be found in the time domain, however, using the memory, or retardation functions [22]. The modified time domain equation of motion to include all radiative effects is:

$$([M]+[A])\{\ddot{\eta}\}+([B]+[B^V]+[B^C])\{\dot{\eta}\}+([C]+[C^C])\{\eta\}$$
$$+\int_{-\infty}^{t}[K(t-\tau)]\{\ddot{\eta}\}d\tau = \{F^I\}+\{F^D\}+\{F^C\}. \tag{35}$$

The elements of the kernel of the integral in the retardation function are found by,

$$K_{jk}(\tau) = \frac{2}{\pi}\int_0^{\infty}(A_{jk}(\omega_e)-A_{jk}(\infty))\cos\omega_e\tau d\omega_e, \text{ or} \tag{36}$$

$$K_{jk}(\tau) = \frac{2}{\pi}\int_0^\infty \frac{B(\omega_e)}{\omega_e}\sin\omega_e\tau d\omega_e . \tag{37}$$

A typical heave memory function for zero speed is shown in Figure 21 (38)

(39)

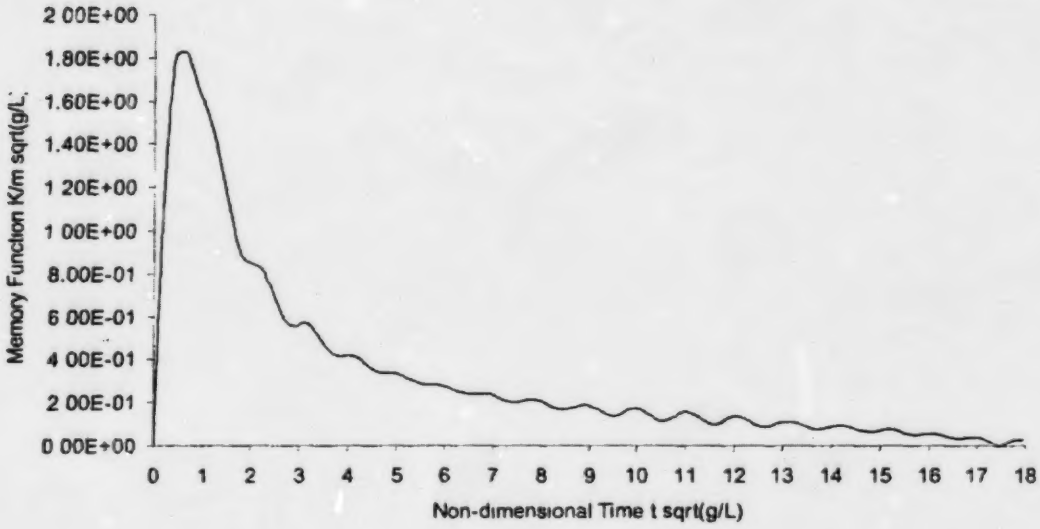

Figure 21: Typical Memory Function for zero speed.

In theory the two definitions are equivalent but through numerical evaluation there may exist some differences. If this approach is used, the kernel of the integrals in eqs. 36-37 must be evaluated for a complete range of frequencies. Using the existing Submo code it is not possible to compute infinite frequencies, however the functions are asymptotic and could be evaluated to a realistic limit. The time dependent integration in eq. 35, must only be evaluated to a characteristic time in history as the K functions repeat and can produce erroneous results. This value of time is dependent on the lower limit of integration for frequency and the frequency step size. Although usually used when forcing functions of a cyclic nature are present, for rigorous modelling in the deeply submerged case, the memory function should be included. The current report does not detail the coding of such an addition to manoeuvring models.

4.0 Time Domain Code Verification

4.1 Linear Time Domain Verification Theory

There are various methods and formats for a time domain model structure. In order to check the output of the three routines described previously, some kind of model is needed. The equation of

motion as given by eq. 1 is used in combination with the dummy variable ζ, so that the equations can be written:

$$([M]+[A])\{\dot{\zeta}\}+([B]+[B^V]+[B^C])\{\zeta\}+([C]+[C^C])\{\eta\} = \{F^E\} \tag{40}$$

$$\{\zeta\} = \{\dot{\eta}\} \tag{41}$$

Then the two differential equations can be combined to one first order set of differential equations:

$$\begin{bmatrix}\{\dot{\zeta}\}\\ \{\dot{\eta}\}\end{bmatrix} = \begin{bmatrix}([M]+[A])^{-1}(\{F^E\}-([B]+[B^V]+[B^C])\{\zeta\}-([C]+[C^C])\{\eta\})\\ \{\zeta\}\end{bmatrix} \tag{42}$$

In this way the linear set of differential equations can be integrated. The memory functions described by eq. 36-37 are omitted for simplicity and speed of calculation. A numerical fourth order Runge-Kutta integrator [23], was used. A Bretschneider wave spectrum is used for the forcing function as generated by the routine "wvamp".

A number of issues arise in the construction of this simulation. Hydrodynamic added mass and damping values are needed to complete the model. Usually, as mentioned, the infinite frequency added mass and damping values are used in a manoeuvring model. However, this would result in extremely small damping due to the neglect of viscous terms. As such, the added mass and damping corresponding to the average frequency, based on the energy spectrum, is calculated using the relation [9]:

$$T_\omega = \frac{1}{0.773} \times T_P. \tag{43}$$

The next issue is due to the limitations of strip theory. Having determined the values associated with eq. 42, a stability test of the open loop system was performed by checking the eigenvalues of the system. It was found that for high speeds and low frequencies, that the system becomes unstable. After removing the heave and pitch coupling terms the system stability was restored. It was also found that for high speeds, the coupling terms for other modes induce error in results. This is discussed in the next section.

Before beginning simulation it is necessary to set the initial conditions for integration of the differential equations. As the sea state in question is random, and calculation of the response at any instant, including the initial state is not explicit, the definition of exact initial conditions is difficult. It is more practical to set the initial conditions as the linearized state, and allow for a settling of the response. If this method is implemented it is also advised that the wave forces are ramped up to their actual values during the initial simulation time (~ 20-30 peak wave periods).

Most of the problems in the comparison of time domain to frequency domain theory are due to the fact that a response frequency and shape is assumed in frequency domain analysis, whereas in the time domain the response is not defined. This is manifest in the sway and yaw modes in time domain simulation. As there are no restoring or "C" terms associated with these modes, there are no forces to maintain the corresponding response about some linearized or equilibrium value. To

circumvent this problem, it may be necessary to impose a fictitious stiffness term in time domain simulations.

4.2 Results

Verification of the time domain subroutines was performed using the method described above. Although the linear model is simple in structure, many effects were observed in the results produced. Two hull forms were tested, an ellipsoid and Series - 60 hull as described in Section 5 of this report. For each hull form, two speeds, Froude number 0.05, and 0.2 were examined. Also, three headings, 90, 135, and 180 degrees were used.

The appropriate initial conditions and differential equations were used as described in the preceeding paragraphs. Submo was used to generate added mass and damping values for the average spectral frequency. Simulation was performed using a 0.05 second fixed step size for 25 simulated minutes. Good results can be obtained for any step size less than 0.1 seconds. The first 5 simulated minutes were allowed for system settling. Wave forces were ramped up to their actual values during the first 2-3 minutes. For the sway and heave modes, a fictitious stiffness term was added using a natural frequency value based on ~10% of the peak wave encounter frequency. As the system dynamics will change due to the added restoring term, the damping for these modes was corrected for the new stiffness. This is considered a low frequency addition such that results will not be significantly affected. The natural frequencies of other modes were found to be approximately twice the peak encounter frequency.

As the wave forces generated by the subroutines are based on a mean body reference frame, motions were transformed using the linearized heading to the inertial frame. Also, calls to the subroutines were done using values projected onto the linearized trajectory. It was found that the wave forces are highly sensitive to small changes in vehicle depth, location, and heading relative to the waves. It is suggested that a translating mean depth, location, and heading be used in determining wave forces. This can be accomplished using a type of moving average scheme. It may also be advantageous to use a larger time step in the simulation of wave forces than that used for simulation of vehicle motions. After simulation using mean values, the higher order effects such as types of drift can be compared if instantaneous values are used.

Sea state 3 is modelled with a Bretschneider spectrum using a significant wave height of 0.88 m and a peak period of 7.5 sec while sea state 4 uses a significant wave height of 1.88 m and a peak period of 8.8 sec. The results of the ellipsoid simulations are shown in Figures 22-45. Series 60 results are shown in Figures 46-69. Results show root mean square values for displacement and acceleration in translational modes and displacements of all modes of motion. The figures showing surge velocity and heading angle graph the root mean square of the deviation of these states from the equilibrium condition.

All simulations were performed with no coupling terms included. It was found that sway, yaw, roll coupling generally reduced the roll rms values but increased sway and yaw, and had larger effects at higher speeds. This could be linked to the stability seen by removing heave and pitch coupling by the following reasons. From the results shown, roll response is consistently over predicted by the time domain simulation. As roll added mass does not change significantly, this implies that roll damping was under-estimated. As roll damping is found in Submo by iteration, both the initial and final iterations were compared with minor effect on the over prediction in the time domain. For the

ellipsoid shape there are significant differences in the results produced from the three programs. Roll stiffness remains fixed and is calculated from the moments about the water-plane area. The increase in sway and yaw when coupled with roll is due to their effective damping of the roll motions. The time domain simulations show unrealistically large predictions of roll for the Series 60 hull shape. Pitch is also overprediced for some cases in the Series 60 results. This could be due to the heave and pitch coupling stiffness terms which were not included. Thus, for the ellipsoid shape, where pitch and heave coupling should be zero, the time domain predictions are closer to the frequency domain predictions.

For the range of directions and speeds shown, the results compare well with both Shipmo7 and Submo3. As expected some minor deviations are present due to the use of hydrodynamic terms for a single frequency rather than the use of memory functions. Also differences are expected due to decoupling and the time varying trajectory of the vessel in relation to waves. Minor discrepancies could also be due to the added stiffness in sway and yaw.

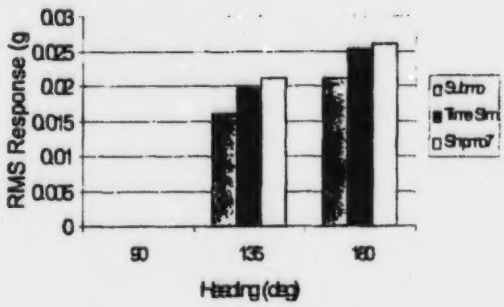

Figure 22: Ellipsoid Time Domain Verification, RMS Surge Acceleration, Sea State 3, Fn .05

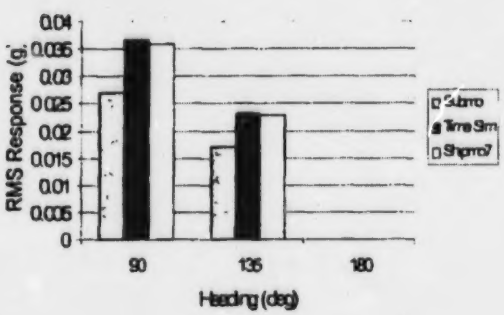

Figure 23: Ellipsoid Time Domain Verification, RMS Sway Acceleration, Sea State 3, Fn .05

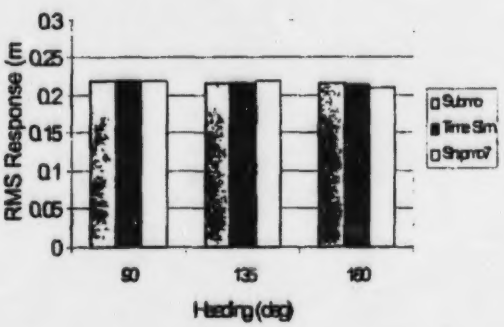

Figure 24: Ellipsoid Time Domain Verification, RMS Heave Displacement, Sea State 3, Fn .05

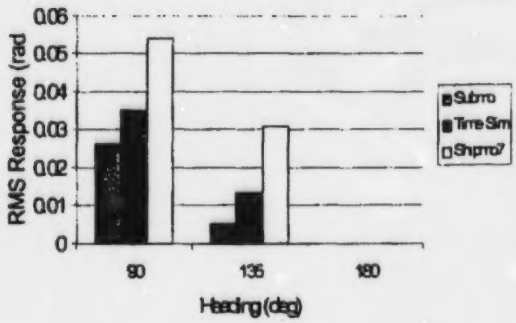

Figure 25: Ellipsoid Time Domain Verification, RMS Roll Displacement, Sea State 3, Fn .05

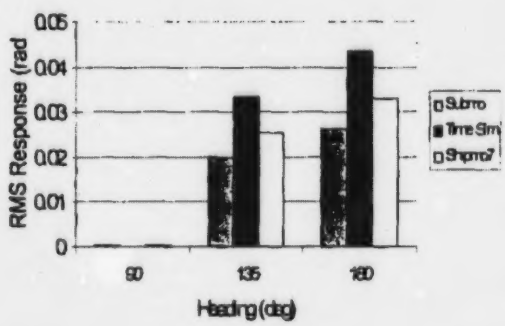

Figure 26: Ellipsoid Time Domain Verification, RMS Pitch Displacement, Sea State 3, Fn .05

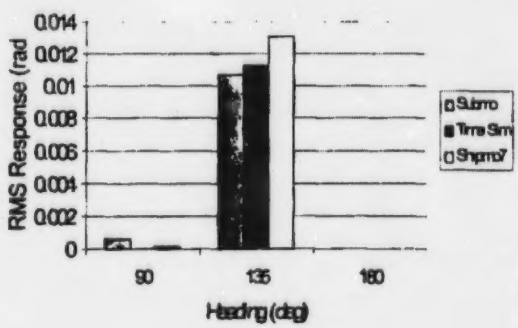

Figure 27: Ellipsoid Time Domain Verification, RMS Yaw Displacement, Sea State 3, Fn .05

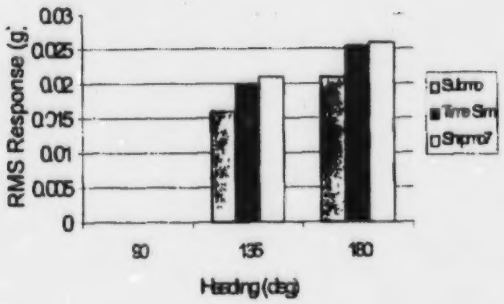

Figure 28: Ellipsoid Time Domain Verification, RMS Surge Acceleration, Sea State 3, Fn 0.2

Figure 29: Ellipsoid Time Domain Verification, RMS Sway Acceleration, Sea State 3, Fn 0.2

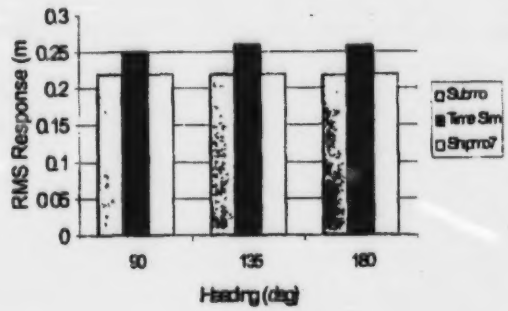

Figure 30: Ellipsoid Time Domain Verification, RMS Heave Displacement, Sea State 3, Fn 0.2

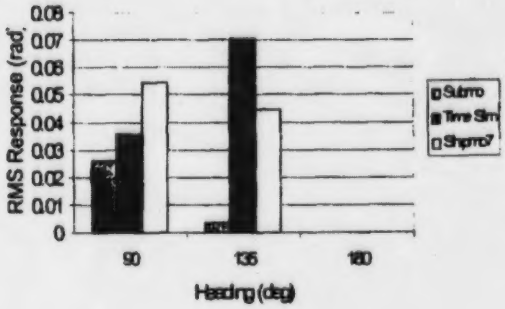

Figure 31: Ellipsoid Time Domain Verification, RMS Roll Displacement, Sea State 3, Fn 0.2

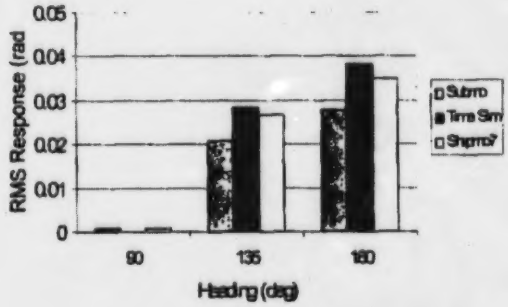

Figure 32: Ellipsoid Time Domain Verification, RMS Pitch Displacement, Sea State 3, Fn 0.2

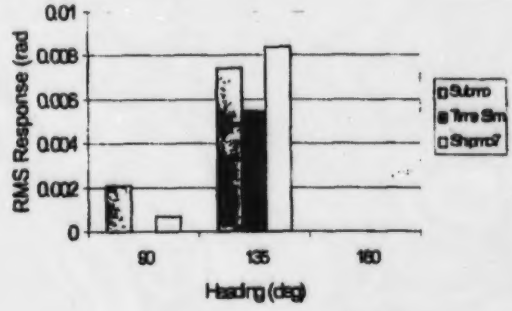

Figure 33: Ellipsoid Time Domain Verification, RMS Yaw Displacement, Sea State 3, Fn 0.2

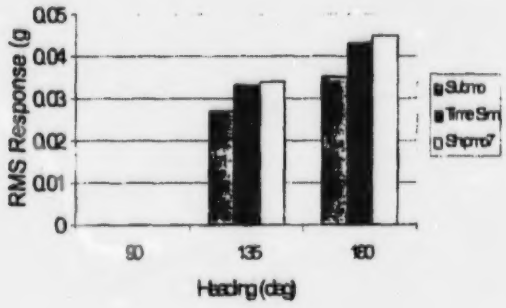

Figure 34: Ellipsoid Time Domain Verification, RMS Surge Acceleration, Sea State 4, Fn .05

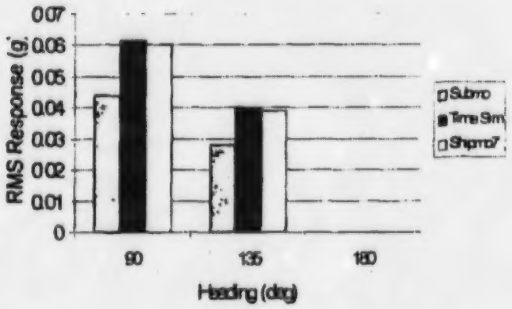

Figure 35: Ellipsoid Time Domain Verification, RMS Sway Acceleration, Sea State 4, Fn .05

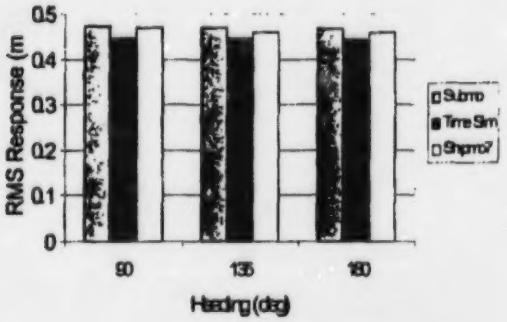

Figure 36: Ellipsoid Time Domain Verification, RMS Heave Displacement, Sea State 4, Fn .05

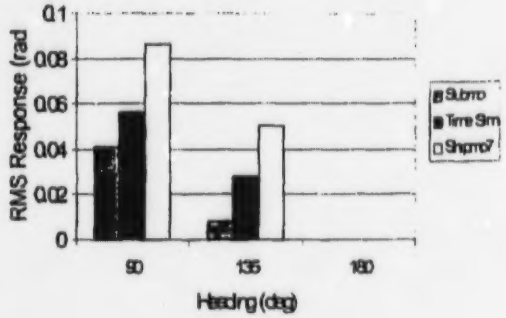

Figure 37: Ellipsoid Time Domain Verification, RMS Roll Displacement, Sea State 4, Fn .05

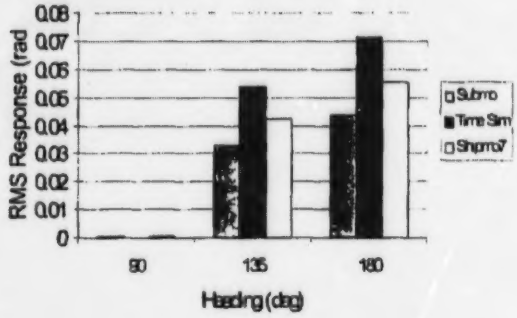

Figure 38: Ellipsoid Time Domain Verification, RMS Pitch Displacement, Sea State 4, Fn .05

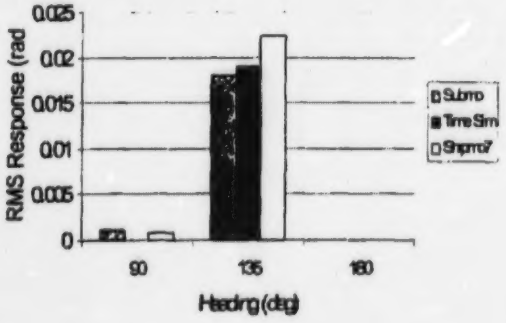

Figure 39: Ellipsoid Time Domain Verification, RMS Yaw Displacement, Sea State 4, Fn .05

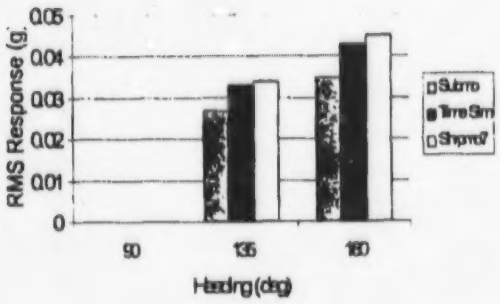

Figure 40: Ellipsoid Time Domain Verification, RMS Surge Acceleration, Sea State 4, Fn 0.2

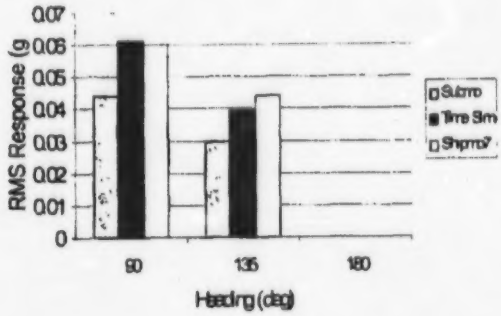

Figure 41: Ellipsoid Time Domain Verification, RMS Sway Acceleration, Sea State 4, Fn 0.2

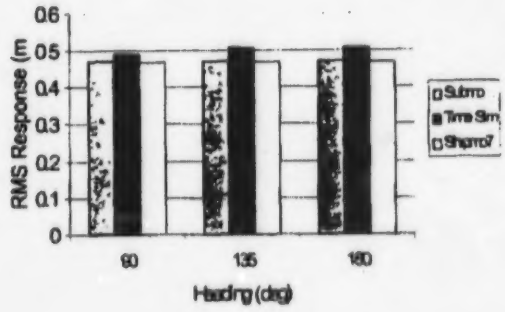

Figure 42: Ellipsoid Time Domain Verification, RMS Heave Displacement, Sea State 4, Fn 0.2

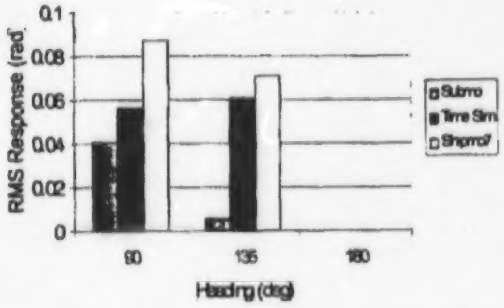

Figure 43: Ellipsoid Time Domain Verification, RMS Roll Displacement, Sea State 4, Fn 0.2

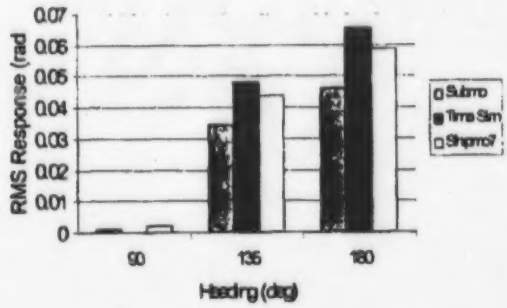

Figure 44: Ellipsoid Time Domain Verification, RMS Pitch Displacement, Sea State 4, Fn 0.2

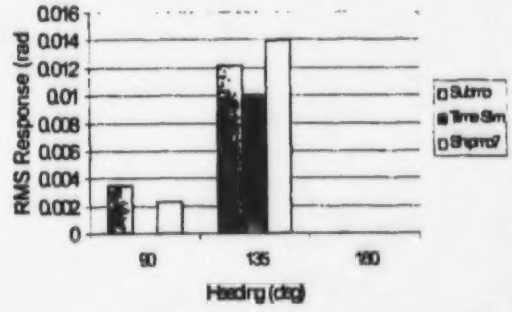

Figure 45: Ellipsoid Time Domain Verification, RMS Yaw Displacement, Sea State 4, Fn 0.2

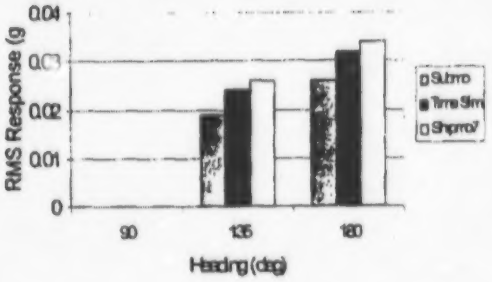

Figure 46: Series 60 Time Domain Verification, RMS Surge Acceleration, Sea State 3, Fn .05

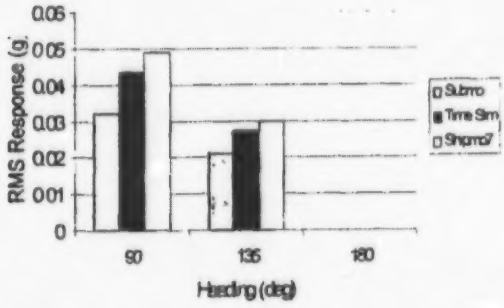

Figure 47: Series 60 Time Domain Verification, RMS Sway Acceleration, Sea State 3, Fn .05

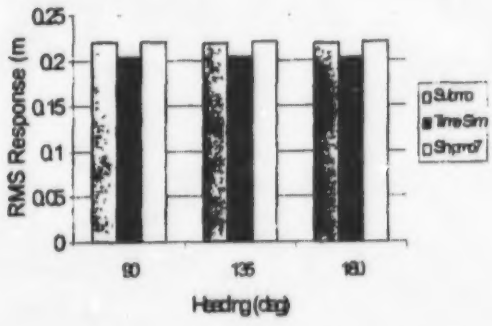

Figure 48: Series 60 Time Domain Verification, RMS Heave Displacement, Sea State 3, Fn .05

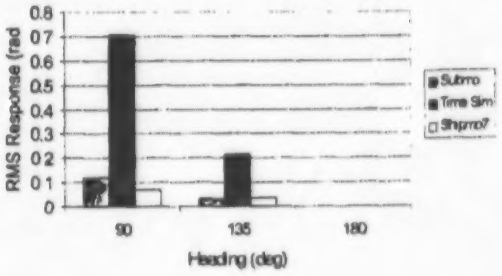

Figure 49: Series 60 Time Domain Verification, RMS Roll Displacement, Sea State 3, Fn .05

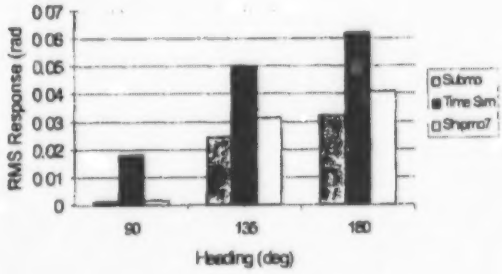

Figure 50: Series 60 Time Domain Verification, RMS Pitch Displacement, Sea State 3, Fn .05

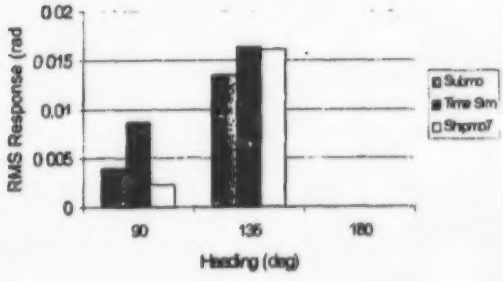

Figure 51: Series 60 Time Domain Verification, RMS Yaw Displacement, Sea State 3, Fn .05

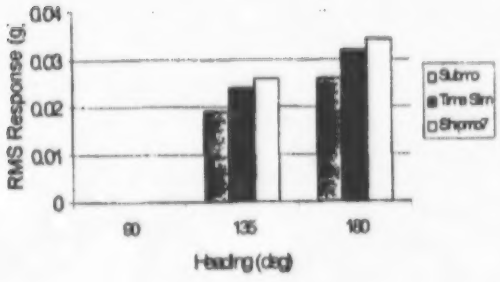

Figure 52: Series 60 Time Domain Verification, RMS Surge Acceleration, Sea State 3, Fn 0.2

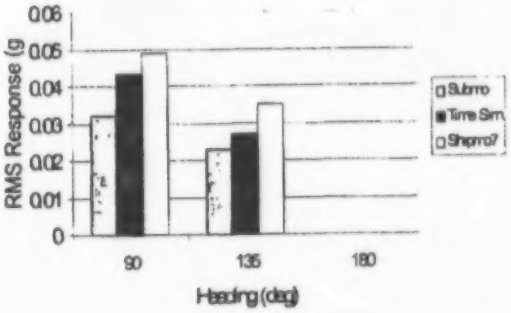

Figure 53: Series 60 Time Domain Verification, RMS Sway Acceleration, Sea State 3, Fn 0.2

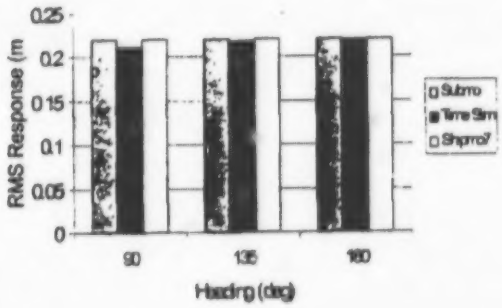

Figure 54: Series 60 Time Domain Verification, RMS Heave Displacement, Sea State 3, Fn 0.2

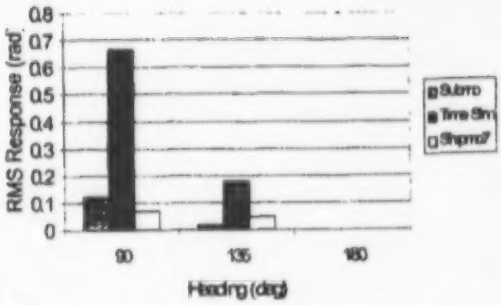

Figure 55: Series 60 Time Domain Verification, RMS Roll Displacement, Sea State 3, Fn 0.2

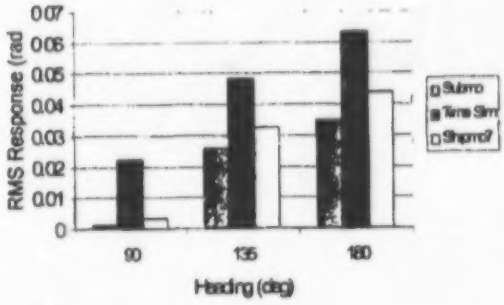

Figure 56: Series 60 Time Domain Verification, RMS Pitch Displacement, Sea State 3, Fn 0.2

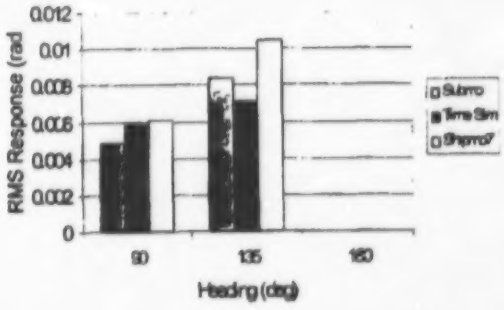

Figure 57: Series 60 Time Domain Verification, RMS Yaw Displacement, Sea State 3, Fn 0.2

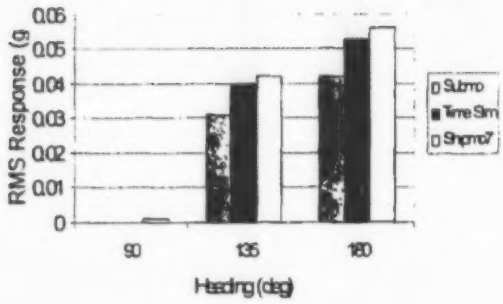

Figure 58: Series 60 Time Domain Verification, RMS Surge Acceleration, Sea State 4, Fn .05

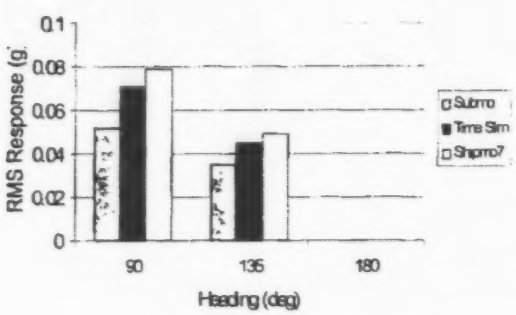

Figure 59: Series 60 Time Domain Verification, RMS Sway Acceleration, Sea State 4, Fn .05

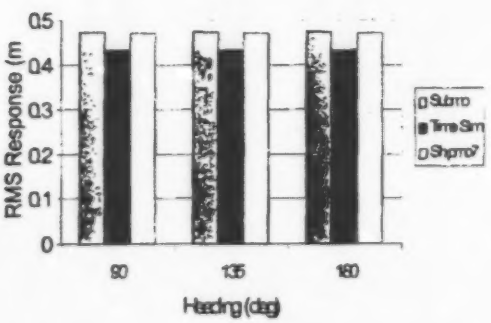

Figure 60: Series 60 Time Domain Verification, RMS Heave Displacement, Sea State 4, Fn .05

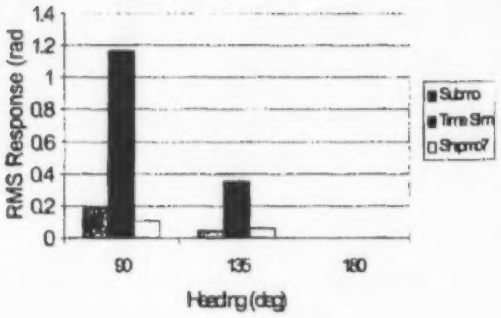

Figure 61: Series 60 Time Domain Verification, RMS Roll Displacement, Sea State 4, Fn .05

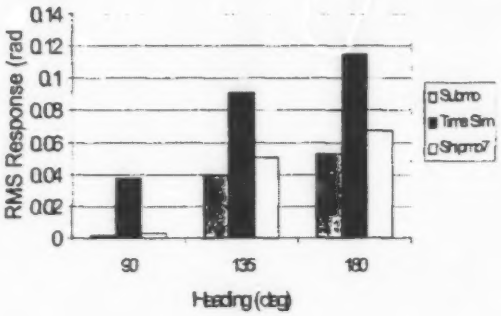

Figure 62: Series 60 Time Domain Verification, RMS Pitch Displacement, Sea State 4, Fn .05

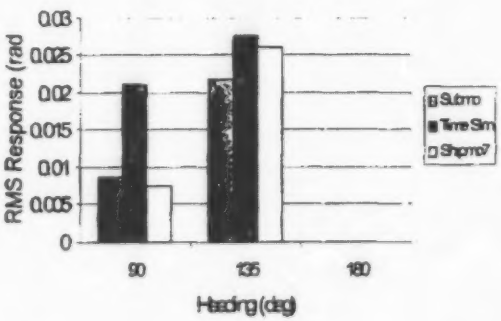

Figure 63: Series 60 Time Domain Verification, RMS Yaw Displacement, Sea State 4, Fn .05

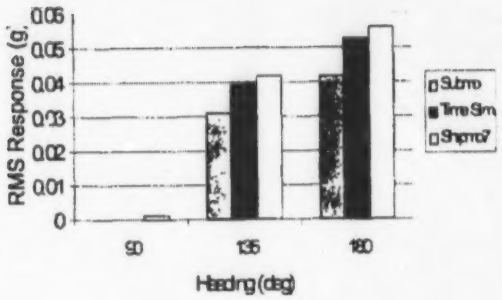

Figure 64: Series 60 Time Domain Verification, RMS Surge Acceleration, Sea State 4, Fn 0.2

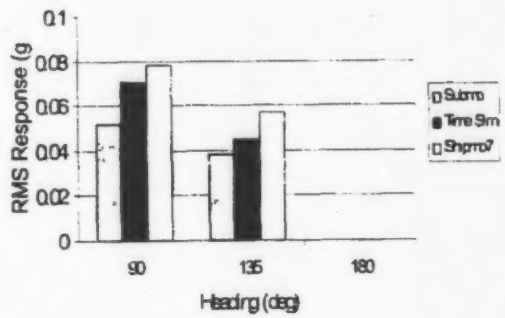

Figure 65: Series 60 Time Domain Verification, RMS Sway Acceleration, Sea State 4, Fn 0.2

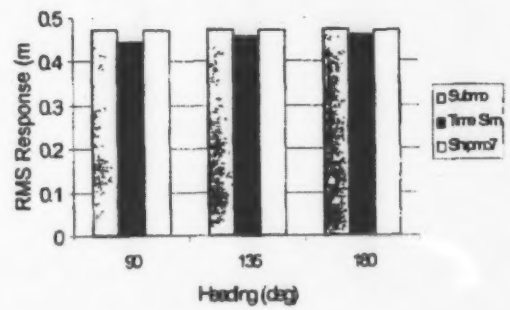

Figure 66: Series 60 Time Domain Verification, RMS Heave Displacement, Sea State 4, Fn 0.2

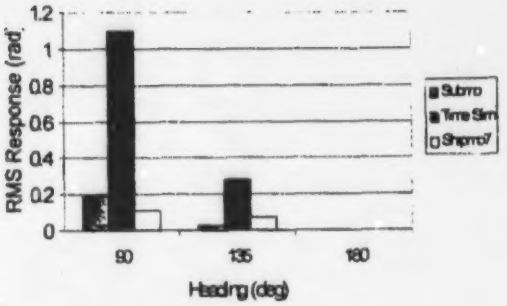

Figure 67: Series 60 Time Domain Verification, RMS Roll Displacement, Sea State 4, Fn 0.2

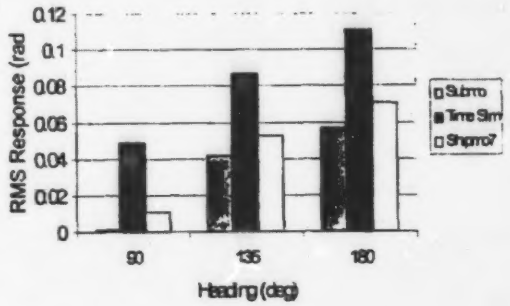

Figure 68: Series 60 Time Domain Verification, RMS Pitch Displacement, Sea State 4, Fn 0.2

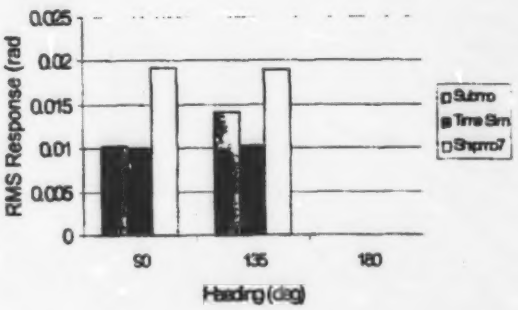

Figure 69: Series 60 Time Domain Verification, RMS Yaw Displacement, Sea State 4, Fn 0.2

5.0 Conclusion

The Submo2 FORTRAN program has been modified using existing theory to include forces and responses in the surge mode. These modifications permit a complete 6 degree of freedom submarine motion simulation in waves. The developments were validated using Shipmo7, and related literature. The Submo predictions shown good agreement with other methods. Surge motions at high frequencies are slightly overpredicted due to diffraction effects. Additional modifications were made to allow the output of frequency dependent wave excitation forces. These force amplitude operators can then be used for time-domain simulation. Generic Fortran 90 Subroutines have been written for the implementation of wave effects in a time domain simulator such as DSSP. Using linear wave theory, a sea state spectrum is found, and the wave excitation forces are constructed using superposition in a cosine series. Additionally, a method for including radiation effects in the time domain is presented. Verification of the subroutines was performed for two geometries and various linearized operating conditions. Most of the time domain results agree well with Submo and Shipmo, however, there are discrepancies in pitch and roll modes for some cases.

6.0 Future Work

The presented work covers an initial approach to calculation of surge motion for a submarine in waves. Diffraction forces in the surge direction are not yet included and could be added by modification of existing Submo routines. In addition, wave making drag, which is included in Shipmo, is not accounted for in Submo. Theoretical methods for calculation of wave drag exist, as well as approximations [24]. However, semi-empirical and experimental formulations are rare. Surface piercing drag effects also may be important in near surface operation and methods are presented here on this topic. Drag effects will usually affect low frequency more than high frequency response.

This work also discusses the transition from frequency domain to time domain simulations. In order to rigorously model the hydrodynamic effects in the time domain, radiative forces must be taken into account. A method for the inclusion of such forces is presented. The comparison between time domain and frequency domain results implies that coupling effects and either the roll hydrodynamics or forcing function be examined in more detail. A good follow up would entail the combination of the wave force subroutines with a more completely developed time domain simulator. Some investigation into coupling effects and phase differences between modes is advised.

7.0 Appendix A - User Information for Subroutines

7.1 Subroutine wvamp(datafile,wf,alpha)

```
Determines wave amplitude data for a given sea spectrum. Assumes unidirectional
long crested seas. This routine must be called once before simulation begins in
order to load spectral and excitation force data.
NOTE:       A regular wave system (spcta=1)
            the Pierson-Moskowitz (spcta=2)
            the Bretschneider (spcta=3)
            the JONSWAP (spcta=4)
            are supported in this version.
Parameters input:
            datafile - name of datafile (from caller)
            wdir - wave direction (deg)(from datafile)
            spcta - type of wave spectra(from datafile)
            wparm1 - first spectral parameter(from datafile)
            wparm2 - second spectral parameter(from datafile)
Parameters output:
            wf - wave frequencies (not encounter)
            alpha - wave amplitudes
All other data is passed to the other subroutines using common blocks. Wvamp
also reads the file "fao.dat" for frequency range data.

Structure of lines in datafile:

wdir spcta seednum
wparam1 wparam2

Definition of variables:

wdir - Wave direction in degrees with respect to inertial frame. (real)
spcta - Index for type of wave spectrum (integer).
seed - Random phase offset seed (integer).
wparam1 - First spectral parameter. For regular waves wparam1 is wave height
(double the amplitude), for Pierson-Moskowitz, Bretschneider and JONSWAP spec-
tra wparam1 is significant wave height (real).
wparam2 - Second spectral parameter. For regular waves wparam2 is wave period,
for Pierson-Moskowitz, Bretschneider and JONSWAP spectra wparam2 is peak wave
period (real).
```

7.2 Subroutine wexfor(t,x,y,z,U,head,wf,alpha,fwave)

```
This routine finds the corresponding exciting force for the vehicle in a given
sea state as a function of time and position. Superposition is assumed so the
total force is the sum of a series of cosine waves with random initial phase
offset. This routine must be called at every time step or derivative step for
higher order integrators.

Input parameters:
      t - time (sec)
      x, y - coordinates of cg rel to inertial frame (m)
      z - location of cg (pos up from mean water line)
```

```
      U - speed over ground (m/s)
      head - heading (deg) rel to inertial frame
      Note: Heading MUST be between 0 and 360 degrees.
      wf - wave frequencies returned from wvamp(rad/sec)
      alpha - wave amplitudes returned from wvamp(m)
Output parameters:
      fwave - instantaneous wave forces and moments (X, Y, Z, K, M, N)
            in Newtons and Newton meters.
```

Note: Best results are obtained if wexfor is called with mean x, y, z and head values averaged over 1-2 times the largest period.

7.3 Subroutine irate(z,U,head,fcomp,pcomp)

This routine interpolates in the array wdata1 for the necessary force amplifiers corresponding to each given frequency. It is called by wexfor.

```
Input paramters:
      z - depth of CG (m, negative down)
      U - forward speed  (m/s)
      head - sub heading (deg. wrt inertial frame
      positive anticlockwise looking at sub from above)
Output parameters:
      fcomp - matrix array of force magnitude operators
      for a given condition size (6 x nwf)
      pcomp - matrix array of relative force phases (6 x nwf)
```

Note: This file only interpolates between speed and heading linearly in matrix form.

7.4 Sample Wave Data File

```
0 3 1
0.88 7.5
```

8.0 Appendix B - Sample Verification Input Files

8.1 Ellipsoid Submo param.dat

```
.805 3.221 2
90. 180. 3
t
3.6652 7 916.3 9162.5 9712.25 0.
3.5 0.0 0.5
0.0 f
0
1000. 1.3e-3
2
0.0 0.0 0.0
3.5 0.0 0.5
2 0.88 7.5
0.5 7.0 37
f t
0
1
```

8.2 Ellipsoid Submo geom.dat

```
17
28 0.388889 0.458100
0.000000 0.270900
0.117300 0.278600
0.164500 0.286200
0.199700 0.293800
0.228600 0.301500
0.253200 0.309100
0.274900 0.316800
0.294100 0.324400
0.311500 0.332000
0.327200 0.339700
0.341500 0.347300
0.354500 0.354900
0.366500 0.362600
0.377500 0.370200
0.387500 0.377800
0.396700 0.385500
0.405200 0.393100
0.412900 0.400700
0.419900 0.408400
0.426200 0.416000
0.431900 0.423600
0.437000 0.431300
0.441500 0.438900
0.445500 0.446600
0.451700 0.461800
0.454000 0.469500
0.455800 0.477100
0.457900 0.492400
```

```
0.458100 0.500000
28 0.777777778 0.6285
0.0 0.185700
0.160900 0.196200
0.225700 0.206700
0.274000 0.217200
0.313600 0.227600
0.347400 0.238100
0.377100 0.248600
0.403600 0.259100
0.427300 0.269500
0.448900 0.280000
0.468500 0.290500
0.486400 0.301000
0.502800 0.311400
0.517900 0.321900
0.531700 0.332400
0.544300 0.342900
0.555900 0.353300
0.566500 0.363800
0.576100 0.374300
0.584800 0.384800
0.592600 0.395200
0.599600 0.405700
0.605800 0.416200
0.611200 0.426700
0.619700 0.447600
0.622900 0.458100
0.625400 0.468600
0.628200 0.489500
0.628500 0.500000
28 1.166667 0.7454
0.0 0.1273
0.1908 0.139700
0.267600 0.152200
0.324900 0.164600
0.371800 0.177000
0.412000 0.189400
0.447200 0.201900
0.478600 0.214300
0.506700 0.226700
0.532300 0.239100
0.555600 0.251500
0.576800 0.264000
0.596300 0.276400
0.614100 0.288800
0.630500 0.301200
0.645500 0.313700
0.659200 0.326100
0.671700 0.338500
0.683100 0.350900
0.693400 0.363400
0.702700 0.375800
0.711000 0.388200
0.718400 0.400600
```

```
0.724800 0.413000
0.734900 0.437900
0.738700 0.450300
0.741600 0.462700
0.744900 0.487600
0.745400 0.500000
28 1.555556 0.8315
0.000000 0.084300
0.2129 0.0981
0.2985 0.112000
0.362400 0.125800
0.414800 0.139700
0.459600 0.153600
0.498900 0.167400
0.533800 0.181300
0.565300 0.195100
0.593800 0.209000
0.619700 0.222800
0.643500 0.236700
0.665200 0.250600
0.685100 0.264400
0.703400 0.278300
0.720100 0.292100
0.735400 0.306000
0.749400 0.319800
0.762100 0.333700
0.773600 0.347600
0.783900 0.361400
0.793200 0.375300
0.801400 0.389100
0.808500 0.403000
0.819800 0.430700
0.824100 0.444600
0.827300 0.458400
0.831000 0.486100
0.831500 0.500000
28 1.944444 0.8958
0.000000 0.052100
0.229400 0.067000
0.3216 0.082
0.3905 0.096900
0.446900 0.111800
0.495200 0.126700
0.537500 0.141700
0.575100 0.156600
0.609000 0.171500
0.639700 0.186500
0.667700 0.201400
0.693200 0.216300
0.716600 0.231300
0.738100 0.246200
0.757800 0.261100
0.775800 0.276000
0.792300 0.291000
0.807300 0.305900
```

```
0.821000 0.320800
0.833400 0.335800
0.844600 0.350700
0.854500 0.365600
0.863400 0.380600
0.871100 0.395500
0.883300 0.425300
0.887800 0.440300
0.891300 0.455200
0.895300 0.485100
0.895800 0.500000
28 2.333333 0.9428
0.000000 0.028600
0.241400 0.044300
0.338500 0.060000
0.411 0.0757
0.4704 0.091400
0.521200 0.107200
0.565700 0.122900
0.605300 0.138600
0.641000 0.154300
0.673300 0.170000
0.702700 0.185700
0.729600 0.201400
0.754200 0.217200
0.776800 0.232900
0.797500 0.248600
0.816500 0.264300
0.833900 0.280000
0.849700 0.295700
0.864100 0.311400
0.877100 0.327200
0.888900 0.342900
0.899400 0.358600
0.908700 0.374300
0.916800 0.390000
0.929600 0.421400
0.934400 0.437100
0.938100 0.452900
0.942300 0.484300
0.942800 0.500000
28 2.722222 0.975
0.000000 0.012500
0.249600 0.028800
0.350000 0.045000
0.425000 0.061300
0.4864 0.0775
0.5389 0.093800
0.585000 0.110000
0.626000 0.126300
0.662900 0.142500
0.696300 0.158800
0.726700 0.175000
0.754500 0.191300
0.780000 0.207500
```

```
0.803300 0.223800
0.824800 0.240000
0.844400 0.256300
0.862300 0.272500
0.878700 0.288800
0.893600 0.305000
0.907100 0.321300
0.919200 0.337500
0.930100 0.353800
0.939700 0.370000
0.948100 0.386300
0.961400 0.418800
0.966300 0.435000
0.970100 0.451300
0.974500 0.483800
0.975000 0.500000
28 3.111111 0.9938
0.000000 0.003100
0.254500 0.019700
0.356800 0.036200
0.433200 0.052800
0.495800 0.069300
0.5493 0.0859
0.5963 0.102500
0.638100 0.119000
0.675700 0.135600
0.709700 0.152200
0.740700 0.168700
0.769100 0.185300
0.795000 0.201900
0.818800 0.218400
0.840700 0.235000
0.860700 0.251500
0.879000 0.268100
0.895700 0.284700
0.910800 0.301200
0.924600 0.317800
0.937000 0.334400
0.948000 0.350900
0.957800 0.367500
0.966400 0.384100
0.979900 0.417200
0.984900 0.433700
0.988800 0.450300
0.993300 0.483400
0.993800 0.500000
28 3.500000 1.0
0.000000 0.000000
0.256000 0.016700
0.359000 0.033300
0.435900 0.050000
0.498900 0.066700
0.552800 0.083300
0.6 0.1
0.642 0.116700
```

```
0.679900 0.133300
0.714100 0.150000
0.745400 0.166700
0.773900 0.183300
0.800000 0.200000
0.823900 0.216700
0.845900 0.233300
0.866000 0.250000
0.884400 0.266700
0.901200 0.283300
0.916500 0.300000
0.930400 0.316700
0.942800 0.333300
0.953900 0.350000
0.963800 0.366700
0.972400 0.383300
0.986000 0.416700
0.991100 0.433300
0.995000 0.450000
0.999400 0.483300
1.000000 0.500000
28 3.888889 0.9938
0.000000 0.003100
0.254500 0.019700
0.356800 0.036200
0.433200 0.052800
0.495800 0.069300
0.549300 0.085900
0.596300 0.102500
0.6381 0.119
0.6757 0.135600
0.709700 0.152200
0.740700 0.168700
0.769100 0.185300
0.795000 0.201900
0.818800 0.218400
0.840700 0.235000
0.860700 0.251500
0.879000 0.268100
0.895700 0.284700
0.910800 0.301200
0.924600 0.317800
0.937000 0.334400
0.948000 0.350900
0.957800 0.367500
0.966400 0.384100
0.979900 0.417200
0.984900 0.433700
0.988800 0.450300
0.993300 0.483400
0.993800 0.500000
28 4.277778 0.975
0.000000 0.012500
0.249600 0.028800
0.350000 0.045000
```

```
0.425000 0.061300
0.486400 0.077500
0.538900 0.093800
0.585000 0.110000
0.626000 0.126300
0.6629 0.1425
0.6963 0.158800
0.726700 0.175000
0.754500 0.191300
0.780000 0.207500
0.803300 0.223800
0.824800 0.240000
0.844400 0.256300
0.862300 0.272500
0.878700 0.288800
0.893600 0.305000
0.907100 0.321300
0.919200 0.337500
0.930100 0.353800
0.939700 0.370000
0.948100 0.386300
0.961400 0.418800
0.966300 0.435000
0.970100 0.451300
0.974500 0.483800
0.975000 0.500000
28 4.666667 0.9428
0.000000 0.028600
0.241400 0.044300
0.338500 0.060000
0.411000 0.075700
0.470400 0.091400
0.521200 0.107200
0.565700 0.122900
0.605300 0.138600
0.641000 0.154300
0.6733 0.17
0.7027 0.185700
0.729600 0.201400
0.754200 0.217200
0.776800 0.232900
0.797500 0.248600
0.816500 0.264300
0.833900 0.280000
0.849700 0.295700
0.864100 0.311400
0.877100 0.327200
0.888900 0.342900
0.899400 0.358600
0.908700 0.374300
0.916800 0.390000
0.929600 0.421400
0.934400 0.437100
0.938100 0.452900
0.942300 0.484300
```

```
0.942800 0.500000
28 5.055556 0.8958
0.000000 0.052100
0.229400 0.067000
0.321600 0.082000
0.390500 0.096900
0.446900 0.111800
0.495200 0.126700
0.537500 0.141700
0.575100 0.156600
0.609000 0.171500
0.639700 0.186500
0.6677 0.2014
0.6932 0.216300
0.716600 0.231300
0.738100 0.246200
0.757800 0.261100
0.775800 0.276000
0.792300 0.291000
0.807300 0.305900
0.821000 0.320800
0.833400 0.335800
0.844600 0.350700
0.854500 0.365600
0.863400 0.380600
0.871100 0.395500
0.883300 0.425300
0.887800 0.440300
0.891300 0.455200
0.895300 0.485100
0.895800 0.500000
28 5.444444 0.8315
0.000000 0.084300
0.212900 0.098100
0.298500 0.112000
0.362400 0.125800
0.414800 0.139700
0.459600 0.153600
0.498900 0.167400
0.533800 0.181300
0.565300 0.195100
0.593800 0.209000
0.619700 0.222800
0.6435 0.2367
0.6652 0.250600
0.685100 0.264400
0.703400 0.278300
0.720100 0.292100
0.735400 0.306000
0.749400 0.319800
0.762100 0.333700
0.773600 0.347600
0.783900 0.361400
0.793200 0.375300
0.801400 0.389100
```

```
0.808500 0.403000
0.819800 0.430700
0.824100 0.444600
0.827300 0.458400
0.831000 0.486100
0.831500 0.500000
28 5.833333 0.7454
0.000000 0.127300
0.190800 0.139700
0.267600 0.152200
0.324900 0.164600
0.371800 0.177000
0.412000 0.189400
0.447200 0.201900
0.478600 0.214300
0.506700 0.226700
0.532300 0.239100
0.555600 0.251500
0.576800 0.264000
0.5963 0.2764
0.6141 0.288800
0.630500 0.301200
0.645500 0.313700
0.659200 0.326100
0.671700 0.338500
0.683100 0.350900
0.693400 0.363400
0.702700 0.375800
0.711000 0.388200
0.718400 0.400600
0.724800 0.413000
0.734900 0.437900
0.738700 0.450300
0.741600 0.462700
0.744900 0.487600
0.745400 0.500000
28 6.222222 0.6285
0.000000 0.185700
0.160900 0.196200
0.225700 0.206700
0.274000 0.217200
0.313600 0.227600
0.347400 0.238100
0.377100 0.248600
0.403600 0.259100
0.427300 0.269500
0.448900 0.280000
0.468500 0.290500
0.486400 0.301000
0.502800 0.311400
0.5179 0.3219
0.5317 0.332400
0.544300 0.342900
0.555900 0.353300
0.566500 0.363800
```

```
0.576100 0.374300
0.584800 0.384800
0.592600 0.395200
0.599600 0.405700
0.605800 0.416200
0.611200 0.426700
0.619700 0.447600
0.622900 0.458100
0.625400 0.468600
0.628200 0.489500
0.628500 0.500000
28 6.611111 0.4581
0.000000 0.270900
0.117300 0.278600
0.164500 0.286200
0.199700 0.293800
0.228600 0.301500
0.253200 0.309100
0.274900 0.316800
0.294100 0.324400
0.311500 0.332000
0.327200 0.339700
0.341500 0.347300
0.354500 0.354900
0.366500 0.362600
0.377500 0.370200
0.3875 0.3778
0.3967 0.385500
0.405200 0.393100
0.412900 0.400700
0.419900 0.408400
0.426200 0.416000
0.431900 0.423600
0.437000 0.431300
0.441500 0.438900
0.445500 0.446600
0.451700 0.461800
0.454000 0.469500
0.455800 0.477100
0.457900 0.492400
0.458100 0.500000
0
```

8.3 Series 60 Submo param.dat

```
.532 2.126 2
90. 180. 3
t
0.162 3.05 4.2137 86.874 65.2276 0.
1.525 0.0.175
0.0 f
-.0007
1000. 1.3e-3
2
0. 0. 0.
1.525 0.0 0.175
2 1.88 8.8
0.5 7.0 37
f t
0
1
```

8.4 Series 60 Submo geom.dat

```
19
6   0.1525   0.0499
0.00000 0.00000
0.00566 0.01307
0.02396 0.04358
0.03442 0.08715
0.04008 0.13073
0.04226 0.17430
0.04989 0.21788
6    0.305   0.1028
0.00000 0.00000
0.02179 0.01307
0.05795 0.04358
0.07625 0.08715
0.08866 0.13073
0.09368 0.17430
0.10283 0.21788
6   0.4575   0.1501
0.00000 0.00000
0.05207 0.01307
0.09803 0.04358
0.11982 0.08715
0.13659 0.13073
0.14269 0.17430
0.15010 0.21788
6     0.61   0.1854
0.00000 0.00000
0.09520 0.01307
0.13616 0.04358
0.15772 0.08715
0.17472 0.13073
0.18016 0.17430
0.18539 0.21788
6   0.7625   0.2065
```

```
0.00000 0.00000
0.14073 0.01307
0.17058 0.04358
0.18648 0.08715
0.20042 0.13073
0.20369 0.17430
0.20652 0.21788
6    0.915   0.2157
0.00000 0.00000
0.18082 0.01307
0.19519 0.04358
0.20521 0.08715
0.21349 0.13073
0.21458 0.17430
0.21567 0.21788
6    1.0675   0.2179
0.00000 0.00000
0.20456 0.01307
0.21131 0.04358
0.21436 0.08715
0.21741 0.13073
0.21785 0.17430
0.21785 0.21788
6      1.22   0.2179
0.00000 0.00000
0.21741 0.01307
0.21785 0.04358
0.21785 0.08715
0.21785 0.13073
0.21785 0.17430
0.21785 0.21788
6    1.3725   0.2179
0.00000 0.00000
0.21785  0.01307
0.21785  0.04358
0.21785  0.08715
0.21785  0.13073
0.21785  0.17430
0.21785  0.21788
6     1.525   0.2179
0.00000  0.00000
0.21785  0.01307
0.21785  0.04358
0.21785  0.08715
0.21785  0.13073
0.21785  0.17430
0.21785  0.21788
6    1.6775   0.2179
0.00000  0.00000
0.21785  0.01307
0.21720  0.04358
0.21763  0.08715
0.21785  0.13073
0.21785  0.17430
0.21785  0.21788
```

```
6      1.83    0.2179
0.00000  0.00000
0.20935  0.01307
0.21306  0.04358
0.21545  0.08715
0.21785  0.13073
0.21785  0.17430
0.21785  0.21788
6    1.9825    0.2179
0.00000  0.00000
0.18626  0.01307
0.19977  0.04358
0.20870  0.08715
0.21785  0.13073
0.21785  0.17430
0.21785  0.21788
6     2.135    0.2174
0.00000  0.00000
0.15358  0.01307
0.17755  0.04358
0.19323  0.08715
0.21349  0.13073
0.21589  0.17430
0.21741  0.21788
6    2.2875    0.2146
0.00000  0.00000
0.11590  0.01307
0.14705  0.04358
0.16731  0.08715
0.20195  0.13073
0.20935  0.17430
0.21458  0.21788
6      2.44    0.2070
0.00000  0.00000
0.07494  0.01307
0.11110  0.04358
0.13180  0.08715
0.17973  0.13073
0.19541  0.17430
0.20696  0.21788
6    2.5925    0.1919
0.00000  0.00000
0.04052  0.01307
0.07363  0.04358
0.09302  0.08715
0.14335  0.13073
0.17167  0.17430
0.19193  0.21788
6     2.745    0.1667
0.00000  0.00000
0.01677  0.01307
0.04183  0.04358
0.05337  0.08715
0.09259  0.13073
0.13376  0.17430
```

```
0.16666  0.21788
6    2.8975   0.1246
0.00000  0.00000
0.00501  0.01307
0.01525  0.04358
0.01939  0.08715
0.03573  0.13073
0.08017  0.17430
0.12461  0.21788
0
```

9.0 References

[1] N. Salvesen, E.O. Tuck, and O. Faltinsen, "Ship Motions and Sea Loads," Trans. Society of Naval Architects and Marine Engineers, vol. 78, 1970.

[2] G.W. Johnston and S.P. Foster, "Frequency Domain Prediction of Submarine Motion in Waves (SUBMO) - Volume 1," DREA Contractor Report CR/91/435, 1991.

[3] S.J. Tinker, "Fluid Memory Effects on the Trajectory of a Submersible," Intl. Shipbuilding Progress, vol.25, 1978.

[4] K.A. McTaggart, G.W. Johnston, W. Campbell, and S.P. Foster, "A Strip Theory Program for Submarine Motions in Waves," Proceedings of the Second Canadian Marine Dynamics Conference. Vancouver, August, 1993, pp. 75-82.

[5] T.H. Havelock, "Wave Resistance Theory and its Application to Ship Problems," Trans. SNAME, v. 59, 1951.

[6] M. Aucher, "Dynamique des Sous-Marins," Sciences et Techniques de l'Armement 4e fascicule, Paris, 1981.

[7] G.D. Watt, M. Seto and T. Brockett, "Hydrodynamic Considerations for Semi-Submersible Minehunting Vehicles," 4th Canadian Marine Dynamics and Structures Conference, Ottawa, 1997.

[8] Hoerner, "Fluid Dynamic Drag," Published by Author, 1958.

[9] K.A. McTaggart and R. Graham, "SHIPMO5: An Updated User`s Manual Incorporating New Wave Spectra and Ship-Referenced Forces," DREA Technical Memorandum 92/212, 1992.

[10] G.W. Johnston and A. Skarsgard, "Frequency Domain Prediction of Submarine Motion in Waves -SUBMO2 User Manual," DREA Contractor Report CR/93/439, 1992.

[11] K.A. McTaggart, "Improved Boundary Element Methods for Predicting Sectional Hydrodynamic Coefficients for Strip Theory Motion Programs," DREA Technical Memorandum 96/243, 1996.

[12] F. H. Todd, "Some Further Experiments on Single-Screw Merchant Ship Forms - Series 60," Trans. SNAME, v.61, 1953.

[13] R.B. Inglis and W.G. Price, "A Three Dimensional Ship Motion Theory: Calculation of Wave Loading and Responses with Forward Speed," Trans. RINA, 1981.

[14] A.E. Baitis and T.R. Applebee, "Comparisons Between Measured and Predicted Surge, Sway and Yaw for LCU 1610 and FF 1006," DTNSRDC SPD-694/01, Bethesda, 1976.

[15] R.T. Schmitke, "Ship Sway, Roll, and Yaw Motions in Oblique Seas," Trans. Society of Naval Architects and Marine Engineers, vol. 78, 1970.

[16] M. St.Denis and W.J. Pierson, "On the Motion of Ships in Confused Seas," Trans. SNAME, v.61, 1953.

[17] P. Solberg, "Submarine Dynamics and Modeling," Industrial Control Center, ICC/2/April, Glasgow, 1992.

[18] M. Mackay, "Predicting the Effect of a Hull Plug on Submarine Manoeuvring Using Semiempirical Methods," Royal Institute of Naval Architects International Symposium, Warship '99, London, 1999.

[19] K.A. McTaggart, "SHIPMO7: An Updated Strip Theory Program for Predicting Ship Motions and Sea Loads in Waves," DREA Technical Memorandum 96/243, 1997.

[20] S.K. Chakrabarti, "Hydrodynamics of Offshore Structures," Springer-Verlag, 1987.

[21] G.D. Watt, "Estimates for the Added Mass of a Multi-Component, Deeply Submerged Vehicle; Part I: Theory and Program Description," DREA Technical Memorandum 88/213, 1988.

[22] C.C. Mei, "Floating Body Dynamics: Diffraction and Radiation," John Wiley and Sons, New York, 1983.

[23] William H. Press et al., "Numerical recipes in C : the art of scientific computing, 2nd Edition," Cambridge University Press, Cambridge. 1992.

[24] R. Bhattacharyya, "Dynamics of Marine Vehicles," John Wiley and Sons, New York, 1978.

UNCLASSIFIED
SECURITY CLASSIFICATION OF FORM
(highest classification of Title, Abstract, Keywords)

DOCUMENT CONTROL DATA

(Security classification of title, body of abstract and indexing annotation must be entered when the overall document is classified)

1 ORIGINATOR (the name and address of the organization preparing the document Organizations for whom the document was prepared, e g Establishment sponsoring a contractor's report, or tasking agency, are entered in section 8)

ISE Research Limited

2 SECURITY CLASSIFICATION (overall security classification of the document including special warning terms if applicable)

Unclassified

3 TITLE (the complete document title as indicated on the title page Its classification should be indicated by the appropriate abbreviation (S,C,R or U) in parentheses after the title)

Submo3: A Frequency Domain Simulation Tool for Submarine Motion in Waves, and Its Use with Maneuvering Models

4 AUTHORS (Last name, first name, middle initial If military, show rank, e g Doe, Maj John E)

Field, Adrian I. ISE Research Limited

5 DATE OF PUBLICATION (month and year of publication of document)

April 2000

6a NO OF PAGES (total containing information Include Annexes, Appendices, etc)

58

6b NO OF REFS (total cited in document)

24

7 DESCRIPTIVE NOTES (the category of the document, e g technical report, technical note or memorandum If appropriate, enter the type of report, e g interim, progress, summary, annual or final Give the inclusive dates when a specific reporting period is covered)

Contractor Report

8 SPONSORING ACTIVITY (the name of the department project office or laboratory sponsoring the research and development Include the address)

Defence Research Establishment Atlantic, 9 Grove Street, P.O. Box 1012, Dartmouth, Nova Scotia, Canada, B2Y 3ZY

9a PROJECT OR GRANT NO (if appropriate, the applicable research and development project or grant number under which the document was written Please specify whether project or grant)

1gb14

9b CONTRACT NO (if appropriate, the applicable number under which the document was written)

10a ORIGINATOR'S DOCUMENT NUMBER (the official document number by which the document is identified by the originating activity This number must be unique to this document)

10b OTHER DOCUMENT NOS (Any other numbers which may be assigned this document either by the originator or by the sponsor)

DREA CR 2000-049

11 DOCUMENT AVAILABILITY (any limitations on further dissemination of the document, other than those imposed by security classification)

(X) Unlimited distribution
( ) Distribution limited to defence departments and defence contractors, further distribution only as approved
( ) Distribution limited to defence departments and Canadian defence contractors, further distribution only as approved
( ) Distribution limited to government departments and agencies, further distribution only as approved
( ) Distribution limited to defence departments, further distribution only as approved
( ) Other (please specify)

12 DOCUMENT ANNOUNCEMENT (any limitation to the bibliographic announcement of this document This will normally correspond to the Document Availability (11) However, where further distribution (beyond the audience specified in 11) is possible, a wider announcement audience may be selected)

UNCLASSIFIED
SECURITY CLASSIFICATION OF FORM

13 ABSTRACT (a brief and factual summary of the document It may also appear elsewhere in the body of the document itself It is highly desirable that the abstract of classified documents be unclassified Each paragraph of the abstract shall begin with an indication of the security classification of the information in the paragraph (unless the document itself is unclassified) represented as (S), (C), (R), or (U) It is not necessary to include here abstracts in both official languages unless the text is bilingual)

This report summarizes the developments made to Submo2 resulting in the more recent version, Submo3. Particular changes include the addition of surge motion characteristics, and the ability to output exciting forces to a data file. These changes result in a complete 6 degree of freedom submarine motion model. The results from the software are validated in this work using an ellipsoid and Series 60 hull form, using Shipmo7 and existing literature. Specific use of the excitation force data file for the addition of wave forces and modelling to existing manoeuvring models, such as DSSP, is also detailed. The software code for wave excitation forces in the time domain has been developed and is presented. The procedures are verified by linear time domain simulation and results are compared with frequency domain results from Submo3 and Shipmo7. A method for frequency dependent radiation effects in the time domain is shown.

14 KEYWORDS, DESCRIPTORS or IDENTIFIERS (technically meaningful terms or short phrases that characterize a document and could be helpful in cataloguing the document They should be selected so that no security classification is required Identifiers, such as equipment model designation, trade name, military project code name, geographic location may also be included If possible keywords should be selected from a published thesaurus e g Thesaurus of Engineering and Scientific Terms (TEST) and that thesaurus-identified If it not possible to select indexing terms which are Unclassified, the classification of each should be indicated as with the title)

frequency domain
maneuvering
ship motions
submarine
surge
time domain
wave forces

UNCLASSIFIED
SECURITY CLASSIFICATION OF FORM